AD-A058 789 AIR FORCE MATERIALS LAB WRIGHT-PATTERSON AFB OHIO F/G 17/5
THALLIUM IODIDE COATINGS FOR POTASSIUM CHLORIDE FOR 9.27 MICROM--ETC(U)
FEB 78 M C OHMER

UNCLASSIFIED AFML-TR-77-157 NL

1 OF 1
AD A058 789



END
DATE FILMED
11-78
DDC

AD A058789

DDC FILE COPY

(14) AFML-TR-77-157

LEVEL II

(2)

(10) melvin C. Ohmer

(6) THALLIUM IODIDE COATINGS FOR POTASSIUM CHLORIDE FOR 9.27 MICROMETERS

Laser and Optical Materials Branch
Electromagnetic Materials Division

DDC
SEP 18 1978
F

(11) Feb[redacted]78 (12) 66p.

TECHNICAL REPORT AFML-TR-77-157

(9) Final Report for Period 1 Mar[redacted]76 - 1 Oct[redacted]77

Approved for public release; distribution unlimited.

(17) 02 (16) 2423

AIR FORCE MATERIALS LABORATORY
AIR FORCE WRIGHT AERONAUTICAL LABORATORIES
AIR FORCE SYSTEMS COMMAND
WRIGHT-PATTERSON AIR FORCE BASE, OHIO 45433

012 320

78 09 5 082

NOTICE

When Government drawings, specifications, or other data are used for any purpose other than in connection with a definitely related Government procurement operation, the United States Government thereby incurs no responsibility nor any obligation whatsoever; and the fact that the government may have formulated, furnished, or in any way supplied the said drawings, specifications, or other data, is not to be regarded by implication or otherwise as in any manner licensing the holder or any other person or corporation, or conveying any rights or permission to manufacture, use, or sell any patented invention that may in any way be related thereto.

This report has been reviewed by the Information Office (OI) and is releasable to the National Technical Information Service (NTIS). At NTIS, it will be available to the general public, including foreign nations.

This technical report has been reviewed and is approved for publication.

Melvin C. Ohmer

MELVIN C. OHMER, Project Engineer

FOR THE COMMANDER

Chief, Laser and Optical Materials Branch
Electromagnetic Materials Division

"If your address has changed, if you wish to be removed from our mailing list, or if the addressee is no longer employed by your organization please notify AFML/LPO ,*W-PAFB, OH 45433 to help us maintain a current mailing list".*

Copies of this report should not be returned unless return is required by security considerations, contractual obligations, or notice on a specific document.

AIR FORCE/56780/7 July 1978 — 250

UNCLASSIFIED

SECURITY CLASSIFICATION OF THIS PAGE (When Data Entered)

REPORT DOCUMENTATION PAGE		READ INSTRUCTIONS BEFORE COMPLETING FORM
1. REPORT NUMBER AFML-TR-77-157	2. GOVT ACCESSION NO.	3. RECIPIENT'S CATALOG NUMBER
4. TITLE (and Subtitle) Thallium Iodide Coatings for Potassium Chloride for 9.27 Micrometers		5. TYPE OF REPORT & PERIOD COVERED Technical Report 1 Mar 76 - 1 Oct 77 6. PERFORMING ORG. REPORT NUMBER
7. AUTHOR(s) Melvin C. Ohmer		8. CONTRACT OR GRANT NUMBER(s) 24230201
9. PERFORMING ORGANIZATION NAME AND ADDRESS Air Force Materials Laboratory (LPO) Air Force Wright Aeronautical Laboratories/AFSC Wright-Patterson, OH 45433		10. PROGRAM ELEMENT, PROJECT, TASK AREA & WORK UNIT NUMBERS 62102F 24230201
11. CONTROLLING OFFICE NAME AND ADDRESS		12. REPORT DATE February 1978 13. NUMBER OF PAGES 66
14. MONITORING AGENCY NAME & ADDRESS(if different from Controlling Office)		15. SECURITY CLASS. (of this report) Unclassified 15a. DECLASSIFICATION/DOWNGRADING SCHEDULE

16. DISTRIBUTION STATEMENT (of this Report)

Approved for public release; distribution unlimited.

17. DISTRIBUTION STATEMENT (of the abstract entered in Block 20, if different from Report)

18. SUPPLEMENTARY NOTES

19. KEY WORDS (Continue on reverse side if necessary and identify by block number)

Thallium Iodide, Potassium Chloride, Sodium Fluoride, Thorium Tetrafluoride, Antireflection Coatings, Catbondioxide Lasers, Infrared Coatings, Equivalent Films, Herpin Films, Sodium Chloride

20. ABSTRACT (Continue on reverse side if necessary and identify by block number)

Five three-layer antireflection coatings for potassium chloride incorporating thallium iodide were investigated. The center layers considered were NaF, ThF_4, and KCl. The coatings were tuned for 9.27 micrometers. The window absorption was typically 0.5%. This is a factor of five over the absorption of state of the art coatings at 10.6 micrometers. This increase in absorption is extremely significant. The power handling capability of a window scales with absorption and these absorption measurements indicate that halide windows for operation

DD FORM 1 JAN 73 1473 EDITION OF 1 NOV 65 IS OBSOLETE

UNCLASSIFIED

SECURITY CLASSIFICATION OF THIS PAGE (When Data Entered)

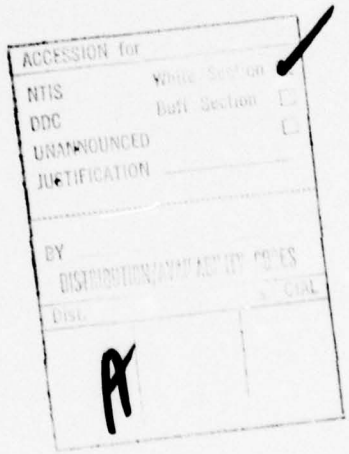
78 09 5 082

at 9.27 micrometers must be significantly derated. Two approaches for systematically investigating possible antireflection coating designs for the case of three layers are presented. One approach utilizes Ohmer's equations (AFML-TR-76-103) for non-integer quarter equivalent films and the other approach utilizes Baer's expressions (Proceedings of 1976 Damage Conference). Author recommends research program on causes of 9.27μm absorption in KCl and development of NaCl for 9.27 micrometers.

FOREWORD

This technical report was prepared by the Air Force Materials Laboratory under Inhouse Work Unit 24230201. Dr. Melvin C. Ohmer was the principal investigator and project engineer for 24230201. The report covers the period 1 March 1976 to 1 October 1977.

The work was performed in the Laser and Optical Materials Branch (LPO), Electromagnetic Materials Division (LP), Air Force Materials Laboratory (AFML).



2

TABLE OF CONTENTS

SECTION		PAGE
I	INTRODUCTION	1
II	PROPERTIES OF THALLIUM IODIDE	7
III	NON-INTEGER QUARTER HERPIN EQUIVALENT APPROACH TO THREE-LAYER DESIGN	14
IV	BAER APPROACH TO THREE-LAYER DESIGN FOR MIDDLE LAYER IDENTICAL WITH SUBSTRATE	30
V	ANHYGROSCOPIC COATING FOR HALIDES	37
VI	EXPERIMENTAL PERFORMANCE OF SOME TlI ANTIREFLECTION COATINGS AT 9.27 MICROMETERS	42
VII	CONCLUSIONS AND RECOMMENDATIONS	50
	REFERENCES	54
	BIBLIOGRAPHY	56

PRECEDING PAGE BLANK

LIST OF ILLUSTRATIONS

FIGURE		PAGE
1	Reflectance vs. Wavelength for $(KCl/TlI)^2$ on Silver for 10.6 Micrometers Courtesy of C. Strecker.	3
2	Thallium Iodide Phase Diagram Taken from Cubicciotti.	8
3	Partial Pressure vs. Temperature for Two Sources of Thallium Iodide Powder Courtesy of G. Blue and E. Rolinski. Pure Denotes Bright Yellow Powder, Gas Denotes Dark Yellow Powder.	10
4	Schuster Diagram Indicating Indices for Which a Solution for Equations 3 and 4 Exist.	16
5	Vector Diagram Depicting: a) Single Layer AR for KCl (n=1.455, .25), b) TlI/KCl (.440/.1583), c) TlI/KCl (.060/.3417).	18
6	Flow Diagram of Equivalent Film Calculation.	20
7	Equivalent Index vs. Film Thicknesses for Thin High Index Solution (7a), Mirror Solution (7b).	22-23
8	Equivalent Index vs. Film Thicknesses for Thick High Index Solution (8a), Mirror Solution (8b).	25-26
9	Vector Diagrams for Four Solutions for N=1.8: a) $+\theta_2$, $+\sin\mu$, b) $-\theta_2$ $+\sin\mu$, c) $-\theta_2$, $-\sin\mu$, d) $+\theta_2$, $-\sin\mu$. Thicknesses Given in Table 6.	27
10	Reduced Optical Thicknesses for Layers 2 and 3 vs. That of Layer 3 in Format of Baer. Radial Lines Indicate Equivalent Index.	29
11	Flow Chart for Baer Calculations.	33
12	Complete Baer Plot for All Four Solutions.	34
13	Comparison of Spectrophotometer Scan for Anhygroscopic Coating (#1256) Before Calorimetry (13a), After Calorimetry at 10.6μm, (13b).	39-40
14	Transmission vs. Wavelength for Design: a) Design 1, b) Design 2, c) Design 3, d) Design 4, e) Design 5, and f) Design 6	47-48

LIST OF TABLES

TABLE		PAGE
1	Major Milestones in the Development of Thallium Iodide	4
2	Thallium Iodide Data Sheet	12
3	Two-Layer Antireflection Coating Thicknesses for Layer One of Thallium Iodide and an Equivalent Outer Layer	19
4	Three-Layer Thicknesses Required for the Thin High Index Solution	21
5	Three-Layer Thicknesses Required for Thick High Index Solution	24
6	Selected Special Solutions to the AR Problem	28
7	Reduced Optical Thickness Obtained from Baer Approach for n = 2.38 and n = 1.455. X Equals Layer 1 etc.	35
8	Properties of Substrates for Anhygroscopic Coating	38
9	Transmission of Anhygroscopic Coating at 9.28μm and 10.6μm	38
10	History Dependent Absorption of Anhygroscopic Coating	41
11	Three-Layer Designs Investigated and Their Deposition Temperature	43
12	Design Indices	43
13	Sample Identification List	44
14	Total Absorption of AR Coated Windows	45
15	Focused Damage Thresholds	46
16	Comparison of 9.27 and 10.6μm Absorption for Samples Described in AFML-TR-77-14	52

SECTION I

INTRODUCTION

The Air Force laser window development program has concentrated on the optimization of polycrystalline doped or alloyed potassium chloride (KCl) for utilization in carbon dioxide laser systems operating at 10.6μm since 1974. Laser windows fail catastrophically by fracture when thermally induced stress exceeds fracture strength as a result of energy absorption. The ultimate limit of applicability of physical laser windows in CW laser systems is determined by the intrinsic absorption limit of transparent materials and the fracture strength attainable in these brittle materials. Therefore, the principle objectives of the program have been to reduce the absorption of KCl to near intrinsic levels, to strengthen KCl by microstructure control, to produce KCl windows of large dimension, to develop polishing and cleaning techniques for KCl which result in a low absorption surface of adequate flatness, and to develop low absorption antireflection coatings for KCl to enhance transmission and protect the hygroscopic KCl from environmental degradation.

Polycrystalline RbCl alloyed KCl has been developed (References 1 and 2) with a fracture strength of 3200 psi and a bulk absorption coefficient of .0005 cm^{-1} at 10.6μm. Surface finishing techniques involving a triacetin slurry of alumina and mechanical chemical-polishing have been developed (Reference 3) for this material which results in a two surface absorption of 1×10^{-4}, surfaces of adequate flatness, and scratch dig numbers better than 15/10. The attainment of high strength in polycrystalline KCl and of low surface absorption on optically finished polycrystalline KCl are major accomplishments of the development program.

After extensive research (References 3, 4, and 5) a thallium iodide-potassium chloride-thallium iodide (Tl/KCl/TlI) three-layer coating was developed for KCl with a very low absorption per surface below the program goal of .04% per surface. During a recent reproducibility demonstration 20 windows (Reference 5) were produced consecutively. Fourteen of these samples had an absorption per surface below 0.02%, five had an

absorption in the range of 0.02 - 0.03% and one had an absorption of 0.037%. For this set of 20 samples, the mean total absorption for a fully coated one-centimeter thick window was 0.09%, the mean substrate absorption was .0006 cm^{-1}, the mean absorption per surface was 0.016% and the mean reflectance per surface was 0.46%. The TlI/KCl/TlI coated KCl windows will pass the scotch tape adhesion test and the cheesecloth abrasion test. They have survived four hours at 70% relative humidity at room temperature. The coatings can be cleaned with xylene. The damage threshold for focused CW CO_2 radiation for the three layer TlI based coating exceeds 130 kw/cm^2 (Reference 6). The threshold for this coating for flood loading of a centimeter spot size exceeds 10 kw/cm^2 at a throughput of 10 kw. Thallium iodide performs well because its thermal expansion coefficient is a perfect match for that of KCl, it deforms plastically, its absorption is immeasurably low, and its solubility in water is substantially below that of KCl. The properties of TlI are extensively treated in Section II. An acceptable CW CO_2 damage threshold for coated KCl appears to depend mainly on attaining a low substrate surface absorption, a low coating absorption, and elimination of stress in coatings stacks which occur during heating rather than for other esoteric reasons (Reference 7). Thallium iodide is readily available from many sources, since it is a component of KRS-5. The development of this excellent coating represents a significant step toward the practical application of hygroscopic halide materials in laser and infrared systems.

Because of the success of TlI in antireflection coatings for KCl there has been an interest in exploring other applications of TlI. A four layer and a six-layer reflecting stack of alternating quarter wave thicknesses of TlI and KCl were deposited on Cervit™ substrates. These mirrors had a consistent damage threshold (Reference 8) of 6 kw/cm^2 for five seconds for a one centimeter spot diameter. This is the highest uniform damage threshold recorded for dielectric mirror on nonmetal substrates. An interesting feature of these mirrors is that their reflectance is nearly 100% between 9 and 11 microns as can be seen in Figure 1. The laser fusion program at Los Alamos has selected NaCl as a CO_2 laser window because its dielectric strength exceeds that of KCl

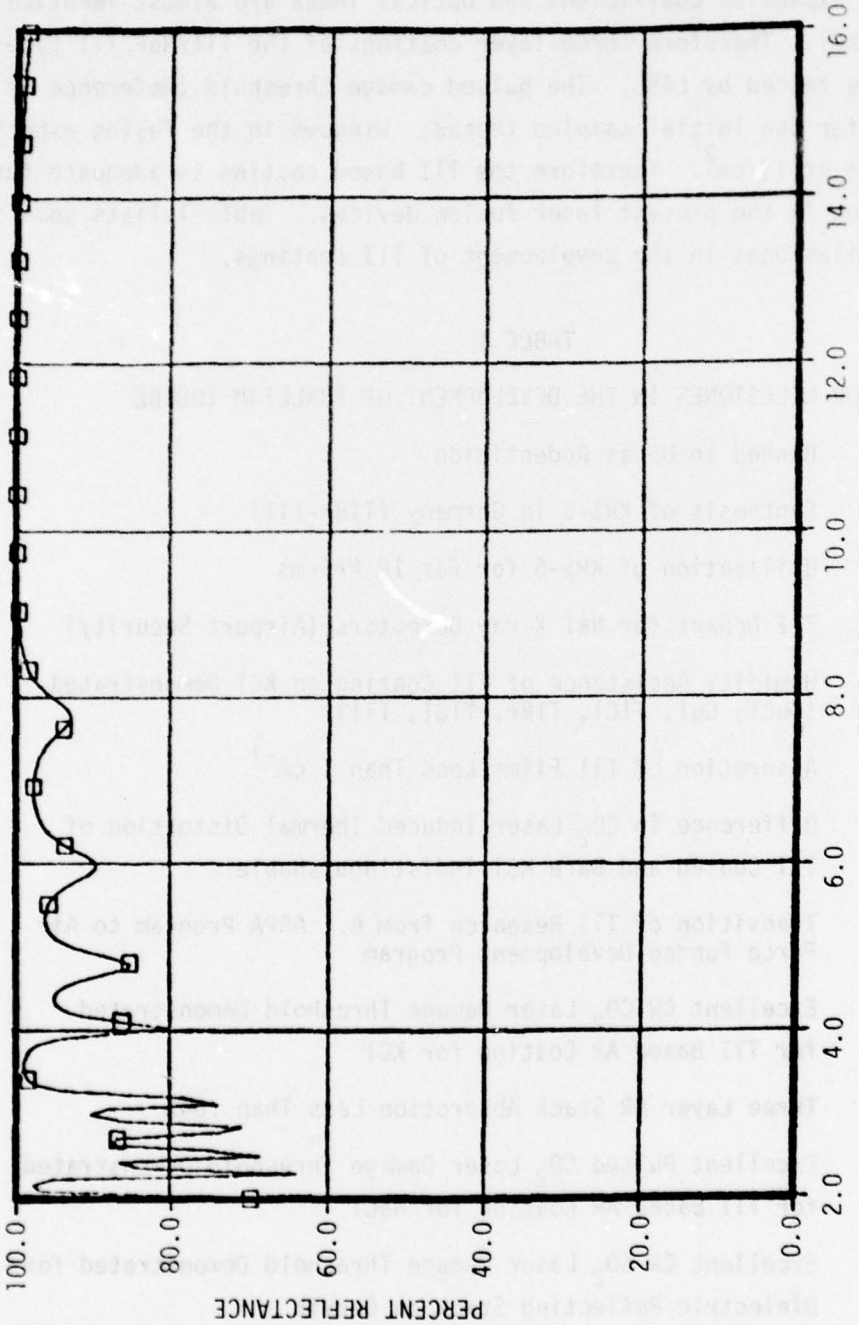


Figure 1. Reflectance vs. Wavelength for $(KCl/TlI)^2$ on Silver for 10.6 Micrometers Courtesy of C. Strecker.

and therefore it has a higher damage threshold in pulsed applications. Its thermal expansion coefficient and optical index are almost identical to that of KCl. Therefore three-layer coatings of the TlI/NaF/TlI type on NaCl were tested by LASL. The pulsed damage threshold (Reference 9) was $3j/cm^2$ for the initial samples tested. Windows in the fusion experiment operate at $1j/cm^2$. Therefore the TlI based coating is adequate for incorporation in the present laser fusion devices. Table 1 lists some of the major milestones in the development of TlI coatings.

TABLE 1

MAJOR MILESTONES IN THE DEVELOPMENT OF THALLIUM IODIDE

1935	Banned in US as Rodenticide
1940's	Synthesis of KRS-5 in Germany (TlBr-TlI)
1947	Utilization of KRS-5 for Far IR Prisms
1970's	TlI Dopant for NaI X-ray Detectors (Airport Security)
1973	Humidity Resistance of TlI Coating on KCl Demonstrated (CuCl, CuI, TlCl, TlBr, TlCl, TlI)
1973	Absorption of TlI Films Less Than 1 cm^{-1}
1974	Difference in CO_2 Laser Induced Thermal Distortion of TlI Coated and Bare KCl Indistinguishable
1975	Transition of TlI Research from 6.1 ARPA Program to Air Force Funded Development Program
1976	Excellent CW CO_2 Laser Damage Threshold Demonstrated for TlI Based AR Coating for KCl
1976	Three Layer AR Stack Absorption Less Than .04%
1977	Excellent Pulsed CO_2 Laser Damage Threshold Demonstrated for TlI Based AR Coating for NaCl
1977	Excellent CW CO_2 Laser Damage Threshold Demonstrated for Dielectric Reflecting Stack on Cervit
1977	Under Consideration as a Coating Material for 17-Inch Diameter Ge Isolators in Fusion Devices

Recently emphasis on windows for CO_2 lasers has shifted from 10.6μm to 9.27μm. Both transitions have the same upper level so there is the same number of photons available at either wavelength. Since the 9.27μm photons are more energetic (E=hν), operating a CO_2 laser at 9.27μm should be 14% more efficient in addition to advantages associated with diffraction limitations. Because of this interest in windows for 9.27μm, TlI/X/TlI coated KCl windows were obtained and evaluated for X=KCl, NaF, and ThF_4. In addition an anhygroscopic AR coating for KCl was evaluated. The performance of these windows at 9.27μm is discussed in detail in Sections V and VI. There is a well documented absorption band (References 10 and 11) typically centered at 9.6μ in many materials. Therefore, it was expected that the absorption at 9.27μm would be substantially larger than that at 10.6μm. This has proved to be the case with window absorptions typically in the range of 0.5%.

In the drive to reduce surface absorption, materials and designs have changed. Thermally suitable high index coatings material for KCl include As_2S_3, As_2Se_3, GeSe alloys, and TlI. For two-layer designs the only low index material which has been seriously considered has been ThF_4. For three-layer designs the low index materials KCl and NaF have been utilized as the central layer. The absorption levels which have been attained with these various coatings range from 0.2% per surface to below 0.04% per surface. While there are usually only two possible two-layer AR coating designs and in rare cases four possible two-layer AR designs for two coating materials there are usually an infinite number of three-layer designs for these materials. It is possible to use design to reduce surface absorption. For example (References 12 and 13), reducing the thickness of the high absorbing material in three-layer designs has enabled the absorption of AR coating stacks incorporating ThF_4 to range below 0.1% per surface to levels of 0.05% per surface. However there are usually an infinite number of coating designs which have adequate optical performance. It has generally been the case that a designer utilizes the first design he is able to construct and in many instances coating designs are selected for no rational reason. A systematic approach for selecting an AR coating design should be considered. For this reason, sample problems utilizing the non-integer equivalent film

approach and the Baer approach are presented in Sections III and IV. A systematic approach treating the approximate problem for the case of zero absorption as in Sections III and IV can provide insight not available from exact optimization methods. Some reasons for selecting a coating design after absorption and reflectance at the design wavelength include environmental durability, balance of thermally induced stress, bandwidth, transmission in the visible, volume of coating material required, and design insensitivity to index. However, ease of fabrication is a very strong selection criteria. A coating design whose thicknesses are appropriate for precise control by an optical thickness monitor may be the best selection.

SECTION II

PROPERTIES OF THALLIUM IODIDE

Thallium iodide received serious consideration as a high index coating material for KCl after Chaffin (Reference 4) demonstrated the stability of a TlI coated KCl surface in high humidity environments and that the absorption of TlI coatings at 10.6μm was below 1 cm^{-1}. TlI has a thermal expansion coefficient nearly identical to that of KCl which allows the deposition of the thick coatings required for IR applications without crazing. TlI films are sometimes cloudy in appearance, a not unusual situation produced by its tendency for oriented growth. However, this cloudiness does not effect its performance in the IR. The report of the cloudy appearance of TlI coatings or possibly its toxic nature may account for the lack of research by the laser window community on TlI coatings for KCl. All research on TlI coatings for KCl prior to 1976 was conducted by Honeywell under ARPA and AFML funded programs. The damage threshold for TlI based AR coatings on KCl for focused 10.6μm radiation was observed to be in excess of 130 kw/cm^2 and for flood loading at 1 cm diameter spot sizes in excess of 10 kw/cm^2. Because of its excellent performance, TlI is the primary candidate for the high index component for AR coatings for KCl.

References 1 and 10 of the bibliography (the original AEC report) by Cubicciotti give the thallium-iodide phase diagram shown in Figure 2. The following comments concerning the phase diagram were taken from the report abstract.

> "There are three compounds: TlI, Tl_3I_4, and TlI_3. From Tl to TlI the solids and liquids are immiscible. From TlI to I_2 there is one liquid phase. Solid Tl_3I_4 melts incongruently at 206°C to a liquid (atom fraction iodine = 0.77) and solid TlI. Solid TlI melts incongruently at 129°C to a liquid (atom fraction iodine = 0.77) and solid TlI. Solid TlI_3 melts incongruently at 129°C to a liquid (atom fraction iodine = 0.84) and solid Tl_3I_4. A eutectic occurs with liquid (atom fraction iodine = 0.88), and solid TlI_3, and solid I_2 at 90°C."

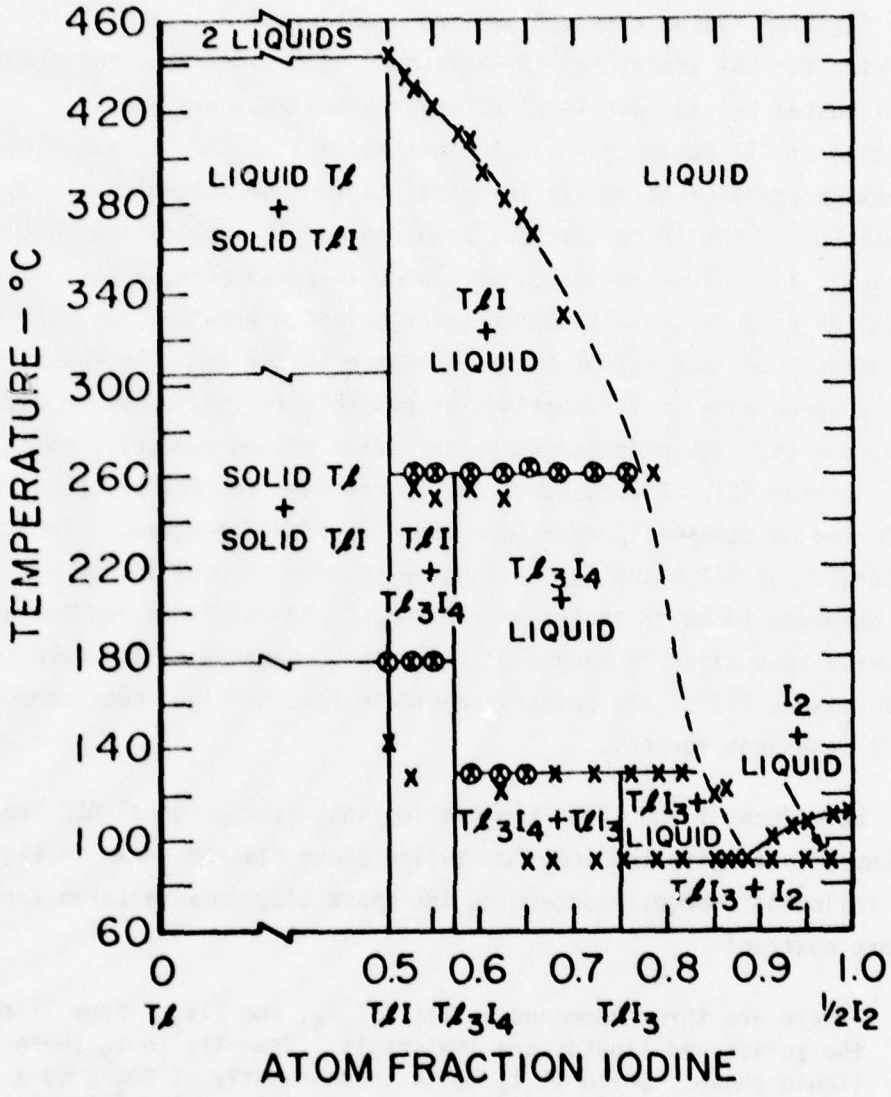


Figure 2. Thallium Iodide Phase Diagram Taken from Cubicciotti.

Consider the compound thallium monoiodide. There are three phases. The low temperature phase is orthorhombic. The temperature of the low temperature phase transition (to a face centered cubic structure) is 170°C. The temperature of the high temperature phase transition to a simple cubic structure is 305°C. Because of this behavior it is better to deposit TlI on room temperature substrates. Figure 2 is of course an equilibrium phase diagram and the orthorhombic to cubic transition can occur at a variety of temperatures as will be discussed in relation to its thermal expansion coefficient. The fcc phase is red, and the orthorhombic phase is yellow. Since the room temperature phase is orthorhombic, the material is birefringent. TlI is a component of KRS-5 a widely used prism material for IR spectrophotometers which is an alloy of TlBr and TlI in the ratio of 2:3. In the alloy the high temperature cubic phase is stabilized. Because of a commercial market for KRS-5, TlI is available from many sources. The purity is usually adequate in all instances except for a problem of excess iodine which must be eliminated in order to achieve low absorption coatings at 10.6μm. If the powder material is bright yellow it is stoichiometric. But if it is yellow-brown in appearance it has excess iodine. Figure 3 is a mass spectrometric comparison (Reference 14) of TlI from two sources. The only difference is the evolution of I_2 gas below 250°C for the yellow-brown powder. No other impurities are observable at sensitivities consistent with high precision mass spectrometry. The evolution of I_2 at low temperature apparently indicates that the iodine is not chemically combined. Recent measurements on the yellow-brown powder utilizing photoacoustic spectroscopy (Reference 15) indicates that the absorption spectrum is that of I_2. It appears that any source of TlI may be used if the material is outgassed in a vacuum system at 250°C. However, one should not use the coating chamber since I_2 can be re-evaporated from the chamber quite readily. The data in Figure 3 indicates the TlI is a molecule in the vapor phase. A small amount of Tl_2I_2 was seen at the higher temperatures. This accounts for the excellent values obtained for absorption in these coatings since stoichiometry is always maintained everywhere. The thermal expansion (Reference 16) of a bulk crystal of TlI obtained from Harshaw of undetermined orientation and crystalline state was measured from room temperature

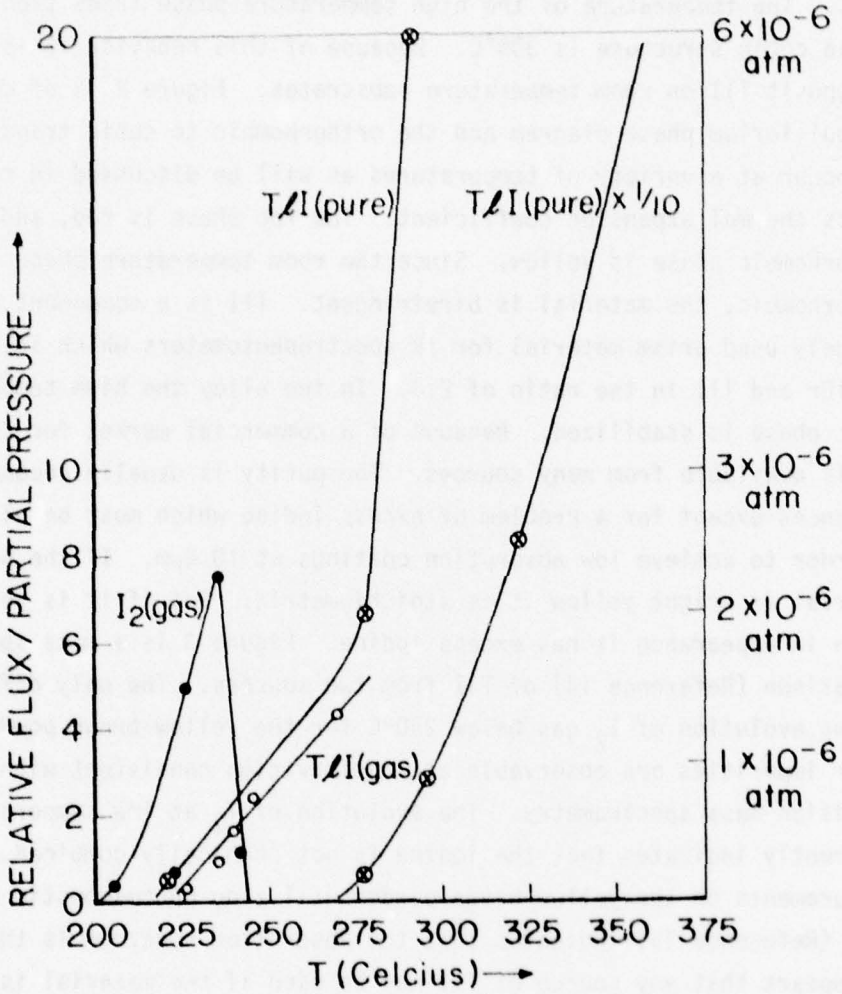


Figure 3. Partial Pressure vs. Temperature for Two Sources of Thallium Iodide Powder Courtesy of G. Blue and E. Rolinski. Pure Denotes Bright Yellow Powder, Gas Denotes Dark Yellow Powder.

to 200°C. At approximately 173°C a discontinuity in the expansion curve occurred due to the orthorhombic to cubic transformation. Below 173°C, the expansion coefficient was 45 x 10^{-6}/°C. The expansion coefficient of the cubic structure was not significantly different. On cooling the discontinuity in thermal expansion did not occur until 125°C. It is fortunate that the discontinuity is well above room temperature. Lowndes and Perry (Reference 17) state that the transformation of TlI to the cubic phase is unusual in a number of ways. The transformation to the cubic phase can be induced by either increasing the temperature or increasing the pressure (i.e., increasing or decreasing cell size). The more symmetric phase is the high temperature phase which is unusual. X-ray data on a number of films have indicated only the orthorhombic phase of TlI. There was no evidence of I_2, Tl_3I_4 or TlI_3. However, asymmetry (Reference 18) observed in the $4f_{7/2}$ Tl ESCA peak indicates the possibility of higher oxidation states of TlI. The question concerning whether a Knudsen cell must be used to evaporate TlI has not been resolved. The ionization potential of 8.46ev would indicate that dissociation by a thermal process should not occur. Some of the samples described in Section VI have been produced by e-beam evaporation; however, there are no one to one comparisons with samples produced using a Knudsen source. Some of the earlier work showing the superiority of the Knudsen source was marred by material problems and possible UV damage of the sample by the source. The problem with a Knudsen source is that it is directional, which makes coating large areas uniformly somewhat difficult. Evile Rutner (Reference 19) has considered the case of extended Knudsen sources. Table 2 contains additional optical, thermal, and mechanical properties of TlI.

TABLE 2

THALLIUM IODIDE DATA SHEET

I. Physical Properties - Bulk

Structure: Orthorhombic (α) for T< 443°K
a_o = 5.251A, b_o = 4.582A, c_o = 12.92Å
Body Centered Cubic (β) for T>443°K
a_o =

Density: α - 7.29g/cm^3 Color: α - Yellow
β - 7.098g/cm^3 β - Red

Solubility in Water: Cold - .0064g/100g H_2O
Hot - .12 g/100g H_2O

Knoop Hardness: As Cut - 27 kg/mm^2
Polished - 8.4 kg/mm^2
Polished and Etched - 8.2 kg/mm^2

II. Physical Properties - Film

Young's Modulus: 2.2 x 10^{5}kg/cm
Stress of Formation: < 50 kg/cm^2
Fracture Stress:
Knoop Hardness:

III. Thermal Properties - Bulk

Thermal Expansion Coefficient: 45 x 10^{-6}/°K - (300-443°K)
Discontinuity at 443°K:
Thermal Diffusivity: .0047 cm^2/sec - (300°K)
Specific Heat: .134 J/(K-gm) @ 300K
Latent Heat of Transformation: (α to β)
Melting Point: 713°K
Boiling Point: 1096°K
Vapor Pressure: $\log_{10}P_{torr}$ = (-0.2185A/T)+B
A = 26789.1
B = 8.247357 440< T< 823°K

T(°K)	$P_{(torr)}$
450	1.74 x 10^{-5}
500	3.47 x 10^{-4}
600	3.10 x 10^{-2}

Ionization Potential: 8.46eV

TABLE 2 (Cont'd)

IV. Thermal Properties - Film

Thermal Expansion Coefficient: $36 \times 10^{-6}/°K$

V. Optical Properties - Bulk

Absorption Edge: .450μm

VI. Optical Properties - Film

Absorption: $\beta < 1\ cm^{-1}$ @ 10.6μm
$4\ cm^{-1}$ @ 9.27μm

Scattering: < .03% for 1μ thickness @ 10.6μm

Index of Refraction:

n	λ
2.49	1.0
2.51	.9
2.55	.8
2.60	.7
2.68	.6

n	λ
2.42 ± .04	1.7 - 10.6μ
2.43	1.6
2.43	1.5
2.44	1.4
2.45	1.3
2.46	1.2
2.51	1.15
2.47	1.1

SECTION III

NON-INTEGER QUARTER HERPIN EQUIVALENT FILMS APPROACH TO THREE LAYER DESIGN

The Herpin non-integer quarter equivalent film technique provides a general building block approach to antireflection coating design. Closed form expressions (Reference 20) for film thicknesses for symmetric three-layer equivalent films for the case of arbitrary equivalent index (N) and phase thickness (μ) are given by Equations 1 and 2 for film stack in the order pqp. The phase thickness and the index of the p layer are respectively ϕ_p and n_p and for the q layer they are respectively ϕ_q and n_q.

$$\sin\phi_q = \frac{\left(n_p/N - N/n_p\right)}{n_p/n_q - n_q/n_p} \sin\mu \qquad (1)$$

Since μ is defined in terms of its cosine, the sign of $\sin\mu$ is undefined. This sign is conventionally chosen so that all real values of N are positive. Equation 1 as a solution for $\sin\mu$ positive and one for $\sin\mu$ negative

$$\sin\left(2\phi_p + \alpha\right) = \frac{c}{r}, \quad \text{for } \begin{matrix} a = r\cos\alpha \\ b = r\sin\alpha \end{matrix}$$

where

$$a = -\frac{1}{2}\left(n_q/n_p + n_p/n_q\right)\sin\phi_q \qquad (2)$$

$$b = \cos\phi_q, \; c = \cos\mu, \; \tan\alpha = b/a.$$

For a high (h) and a low (l) index material it is possible to simulate with the aid of Equations 1 and 2 any intermediate index and any phase thickness when the film stack is ordered hlh or lhl. For 90° films it is possible to simulate indices lower than that of the low index material if the stack is ordered lhl and higher than that of the higher index material if the stack is ordered hlh. As a specific example, 90° films with indices from 0.93 to 3.9 may be simulated using two materials whose indices are 1.5 and 2.42. For equivalent films less than 90° in phase thickness the range of possible indices is even larger because of $\sin\mu$

in Equation 1. In addition, it is even possible to form an equivalent film with an index lower than the lowest in the order of hlh and with an index higher than the highest in the order lhl for thicknesses less than 90°.

A Schuster diagram for possible two-layer AR designs for KCl (extracted from AFML-TR-75-18) is given in Figure 4. This diagram may be used to define the possible three-layer AR designs for the specific case of TlI/KCl/TlI coatings. The line $n_1 = 2.38$ defines all two-layer coatings with an inner layer of TlI. An appropriate outer layer may be constructed in the order hlh for any index less than or equal to 1.973 (corresponds to $n_1/\sqrt{n_s}$), and greater than specified by Equation 1 (i.e. $\sin\phi_q \leq 1$). After selecting the equivalent index of the outer layer (N); the optical thickness of the inner TlI layer θ_1 and that of the outer layer ($\theta_2 = \mu$) may be calculated from Equations 3 and 4. Optical thicknesses for negative angles are obtained adding multiples of π to them.

$$\tan \theta_1 = \frac{\pm n_1^2 (n_o - n_m)(n_m n_o - n_2^2)}{(n_1^2 n_m - n_o n_2^2)(n_o n_m - n_1^2)} \tag{3}$$

$$\tan \theta_2 = \frac{n_2 (n_1^2 - n_o n_m) \tan \theta_1}{n_1 (n_o n_m - n_2^2)} \tag{4}$$

where

n_o = index of refraction of substrate

n_1 = index of refraction of inner or bottom layer

n_2 = index of refraction of outer or top layer

n_m = index of refraction of incident medium

$\theta_1 = \frac{2\pi n_1 t_1}{\lambda}$ = reduced optical thickness

$\theta = \frac{2\pi n_2 t_2}{\lambda}$

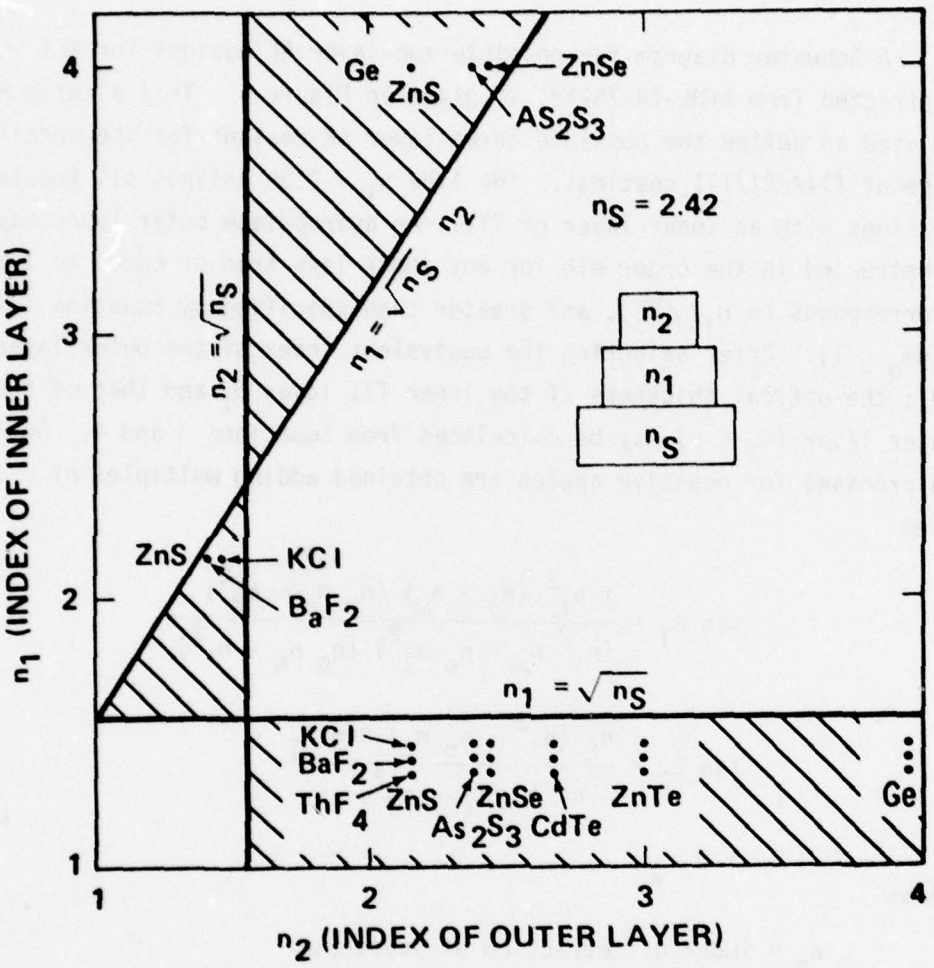


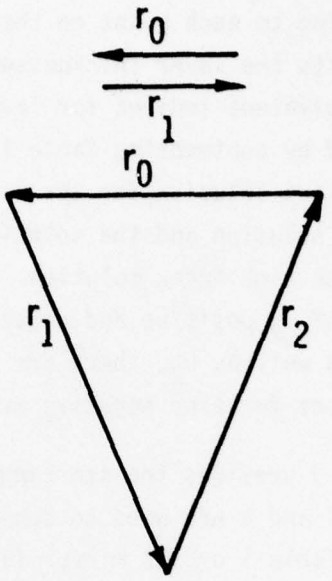
Figure 4. Schuster Diagram Indicating Indices for Which a Solution for Equations 3 and 4 Exist.

Only pairs of indices lying within the shaded region of a Schuster diagram (Figure 4) can be used in Equations 3 and 4. Since Equation 3 yields a positive and a negative value for θ_1, there are two distinct solutions corresponding to each point on the Schuster diagram. For θ_2 positive, Table 3 lists the layer thicknesses for an index of 2.38 for layer 1 and various equivalent indices for layer 2. For θ_2 negative, thicknesses may be obtained by subtracting Table 1 entries from 0.5. In the following discussion the solution for the positive θ_2 is referred to as the thin high index solution and the solution for the negative θ_2 is referred to as the thick high index solution. See Figure 4 for a circle diagram depiction of θ_2 positive and negative. Since $\sin\mu$ may be positive or negative as well as θ_2, there are four solutions for each value of N. The solutions for $\sin\mu$ negative are referred to as mirror solutions.

Table 3 provides the starting point for the three-layer design. Equations 1 and 2 are used to construct the outer layer required by the design in Table 1 or its mirror (i.e. Figure 5c) design using a hlh stack. A flow diagram of the calculation is given in Figure 6. When this stack is added to layer one of the corresponding two-layer design, a three-layer coating results. The three-layer thicknesses required for the thin high index solution are given in Table 4 and are depicted graphically in Figure 7a. Table 5 and Figure 8a give the corresponding information for the thick high index solution. Note that there are four distinct solutions as shown in the circle charts for these designs for N = 1.8 in Figures 9a-9d. The mirror solutions may be obtained by subtracting reduced optical thicknesses for the thin and thick designs from 0.5. They are depicted in Figures 7b and 8b. For the case of n_2 = 2.38 a three-layer design can be found when N is simulated in the order hlh. However no new (Reference 21) distinct solutions are obtained from consideration of this case.

The reduced optical thicknesses for layers 2 and 3 from Tables 4 and 5 have been plotted vs that of layer 1 in Figure 10 in the format of Baer. The figure is divided into two sectors, corresponding to positive and negative θ_1 with positive $\sin\mu$. The arrows indicate the direction of increasing equivalent index. The non-integer Herpin equivalent approach and the approach of Baer yield identical results. A Baer plot of all four solutions is given in Figure 12.

A) $h = \sqrt{n_s}, .25$



B) Tℓ I / KCl
.440 / .158

C) Tℓ I / KCl
.060 / .342

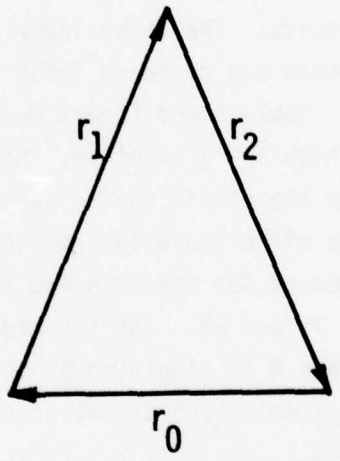


Figure 5. Vector Diagram Depicting: a) Single Layer AR for KCl (n=1.455, .25) b) TlI/KCl (.440/.1583, c) TlI/KCl (.060/.3417).

TABLE 3

TWO-LAYER ANTIREFLECTION COATING THICKNESSES FOR LAYER ONE OF THALLIUM IODIDE AND AN EQUIVALENT OUTER LAYER

N	θ_1	θ_2
1.970	.2327	.2621
1.950	.2032	.2823
1.925	.1834	.2955
1.900	.1689	.3048
1.875	.1572	.3119
1.850	.1472	.3177
1.825	.1384	.3266
1.800	.1306	.3267
1.775	.1234	.3301
1.750	.1168	.3331
1.725	.1107	.3356
1.700	.1050	.3378
1.675	.0996	.3395
1.650	.0945	.3410
1.625	.0896	.3421
1.600	.0849	.3430
1.575	.0804	.3435
1.550	.0760	.3438
1.525	.0717	.3437
1.500	.0675	.3433
1.475	.0633	.3426
1.450	.0592	.3414
1.425	.0551	.3399
1.400	.0510	.3378
1.375	.0468	.3351
1.370	.0459	.3345
1.365	.0451	.3338
1.360	.0442	.3331
1.359	.0440	.3330

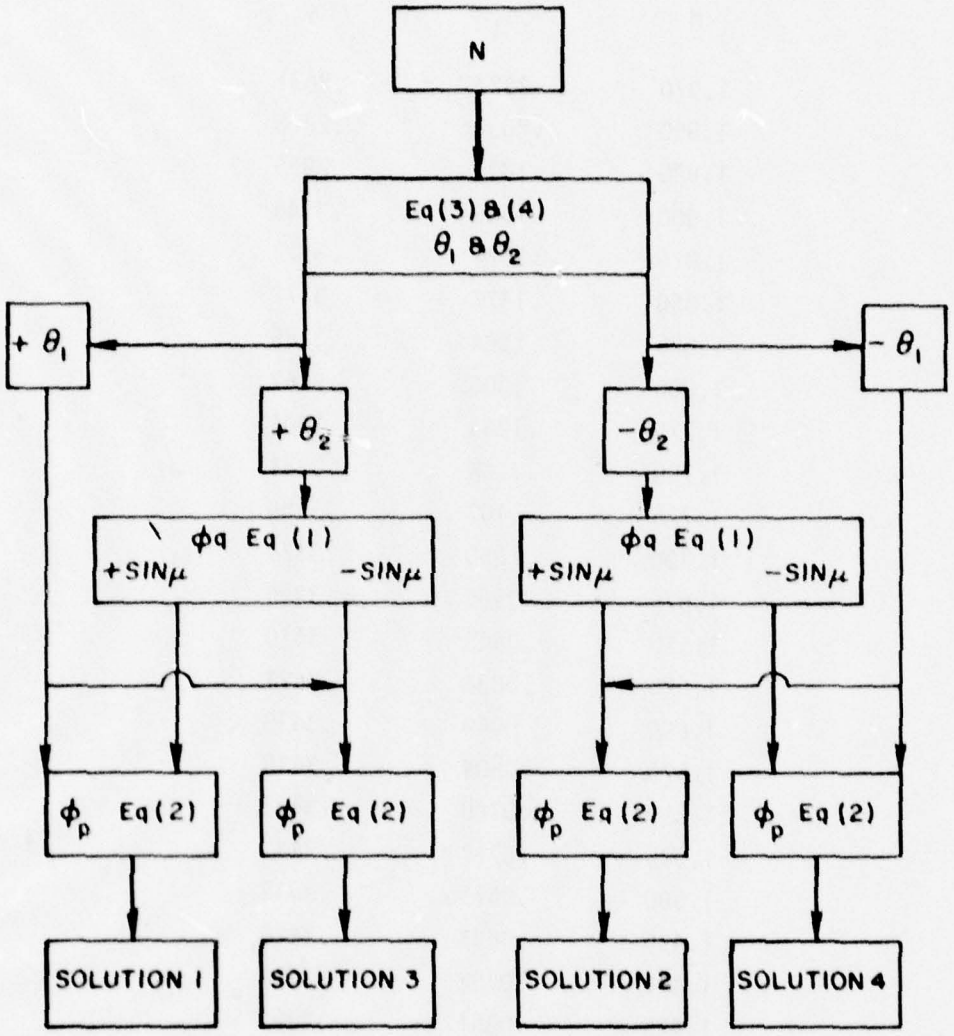


Figure 6. Flow Diagram of Equivalent Film Calculation.

TABLE 4

THREE-LAYER THICKNESSES REQUIRED FOR THE THIN HIGH INDEX SOLUTION

N	ϕ_q layer 2	ϕ_p layer 3	$\theta_1 + \phi_p$ layer 1
1.970	.0604	.0974	.3301
1.950	.0627	.1061	.3093
1.925	.0656	.1110	.2944
1.900	.0685	.1138	.2827
1.875	.0716	.1156	.2728
1.850	.0748	.1167	.2639
1.825	.0780	.1172	.2556
1.800	.0814	.1173	.2479
1.775	.0850	.1170	.2404
1.750	.0886	.1164	.2332
1.725	.0925	.1155	.2262
1.700	.0966	.1142	.2192
1.675	.1009	.1127	.2123
1.650	.1054	.1109	.2054
1.625	.1103	.1088	.1984
1.600	.1155	.1063	.1912
1.575	.1212	.1035	.1839
1.550	.1274	.1003	.1763
1.525	.1342	.0967	.1684
1.500	.1418	.0926	.1601
1.475	.1504	.0878	.1511
1.450	.1605	.0822	.1414
1.424	.1724	.0756	.1307
1.400	.1877	.0673	.1183
1.375	.2100	.0556	.1024
1.370	.2166	.0518	.0977
1.365	.2248	.0483	.0934
1.360	.2380	.0420	.0862
1.359	.2433	.0395	.0835

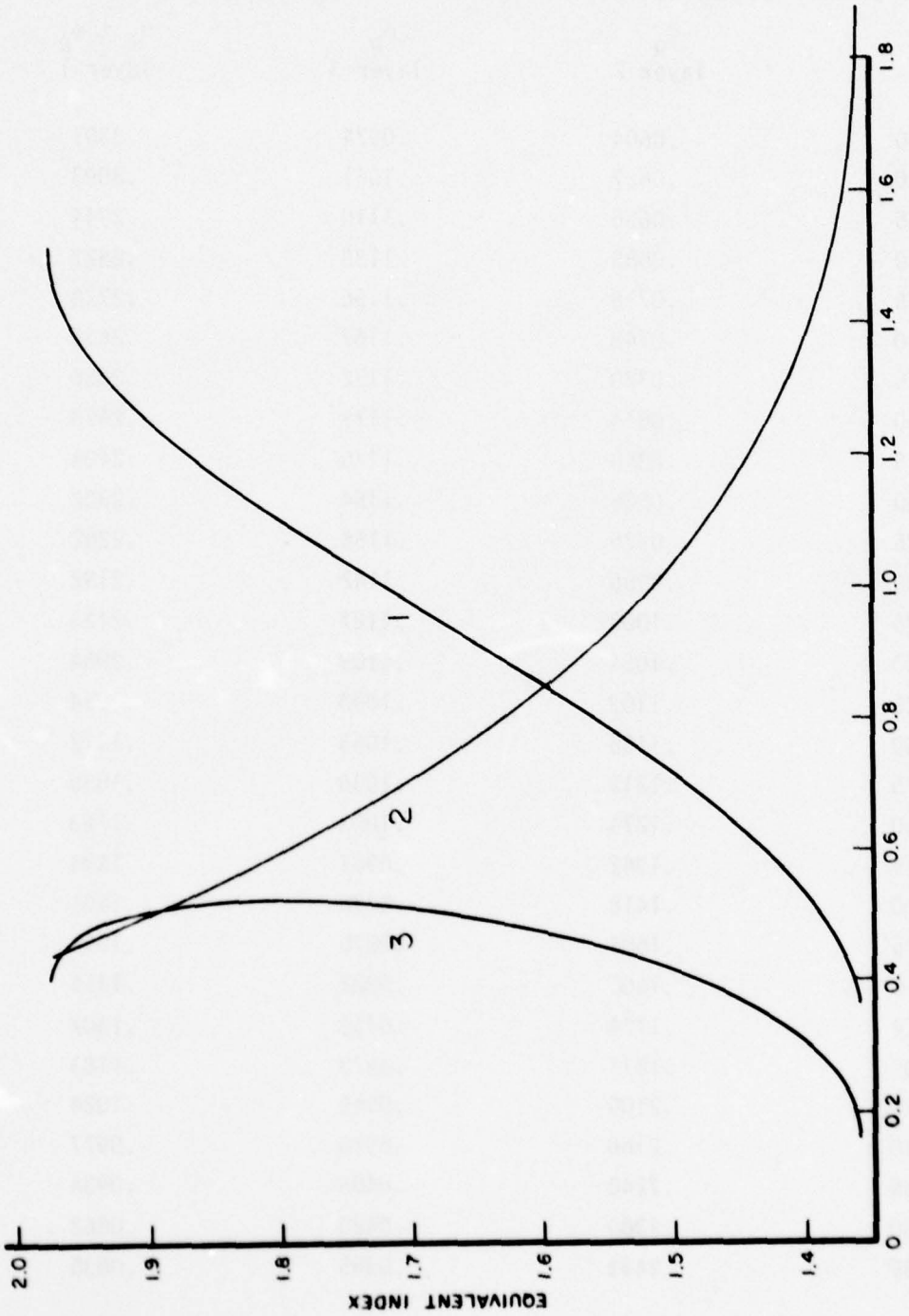


Figure 7a. Equivalent Index vs Film Thicknesses for Thin High Index Solution

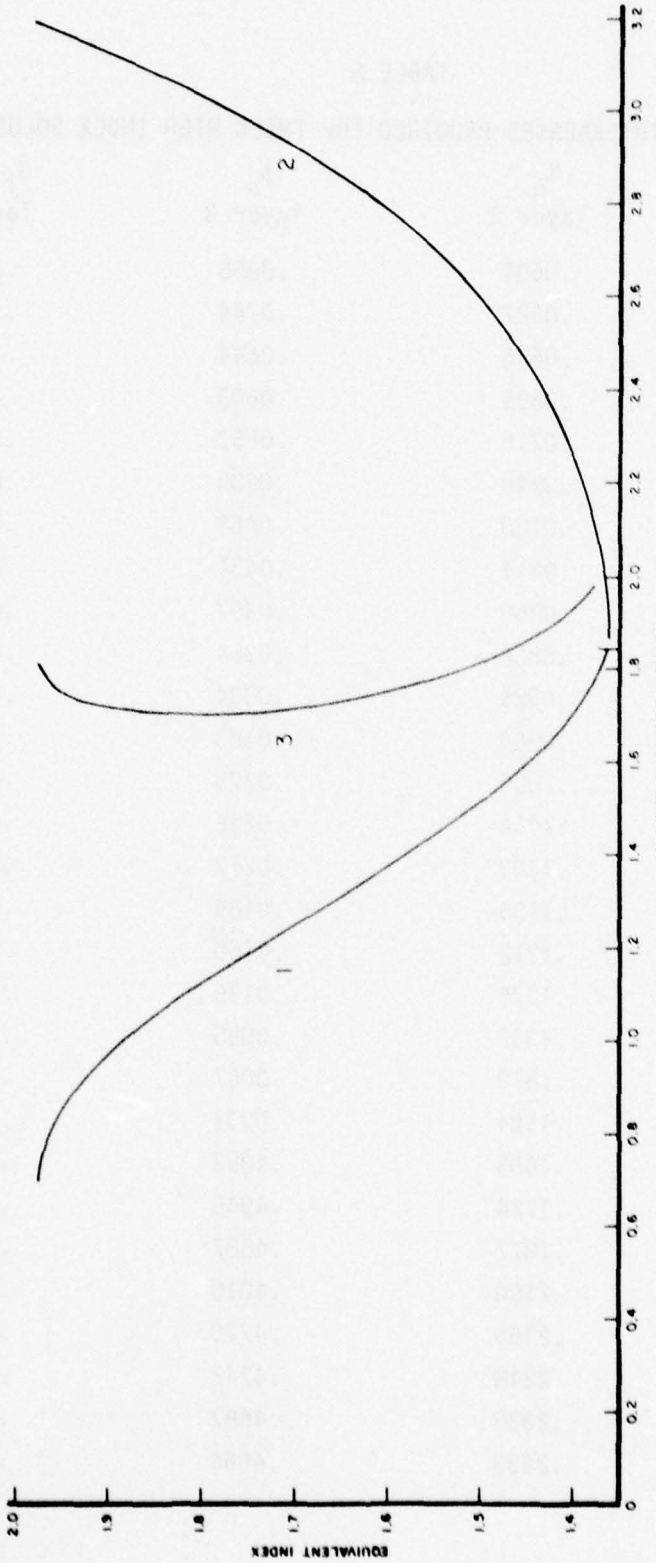


Figure 7b. Equivalent Index vs Film Thicknesses for Mirror Solution

TABLE 5

THREE-LAYER THICKNESSES REQUIRED FOR THICK HIGH INDEX SOLUTION

N	ϕ_q layer 2	ϕ_p layer 3	$\theta_1 + \phi_p$ layer 1
1.970	.0604	.0855	.3528
1.950	.0627	.0744	.3712
1.925	.0656	.0644	.3830
1.900	.0685	.0603	.3914
1.875	.0716	.0553	.3981
1.850	.0748	.0508	.4036
1.825	.0780	.0468	.4084
1.800	.0814	.0431	.4125
1.775	.0850	.0397	.4163
1.750	.0886	.0364	.4196
1.725	.0925	.0334	.4227
1.700	.0966	.0303	.4253
1.675	.1009	.0275	.4279
1.650	.1054	.0246	.4301
1.625	.1103	.0217	.4321
1.600	.1155	.0189	.4340
1.575	.1212	.0160	.4356
1.550	.1275	.0130	.4370
1.525	.1342	.0095	.4378
1.500	.1418	.0067	.4392
1.475	.1504	.0031	.4398
1.450	.1605	.4992	.4400
1.425	.1724	.4945	.4394
1.400	.1877	.4887	.4377
1.375	.2100	.4810	.4333
1.370	.2166	.4775	.4316
1.365	.2248	.4742	.4291
1.360	.2380	.4687	.4245
1.359	.2433	.4664	.4224

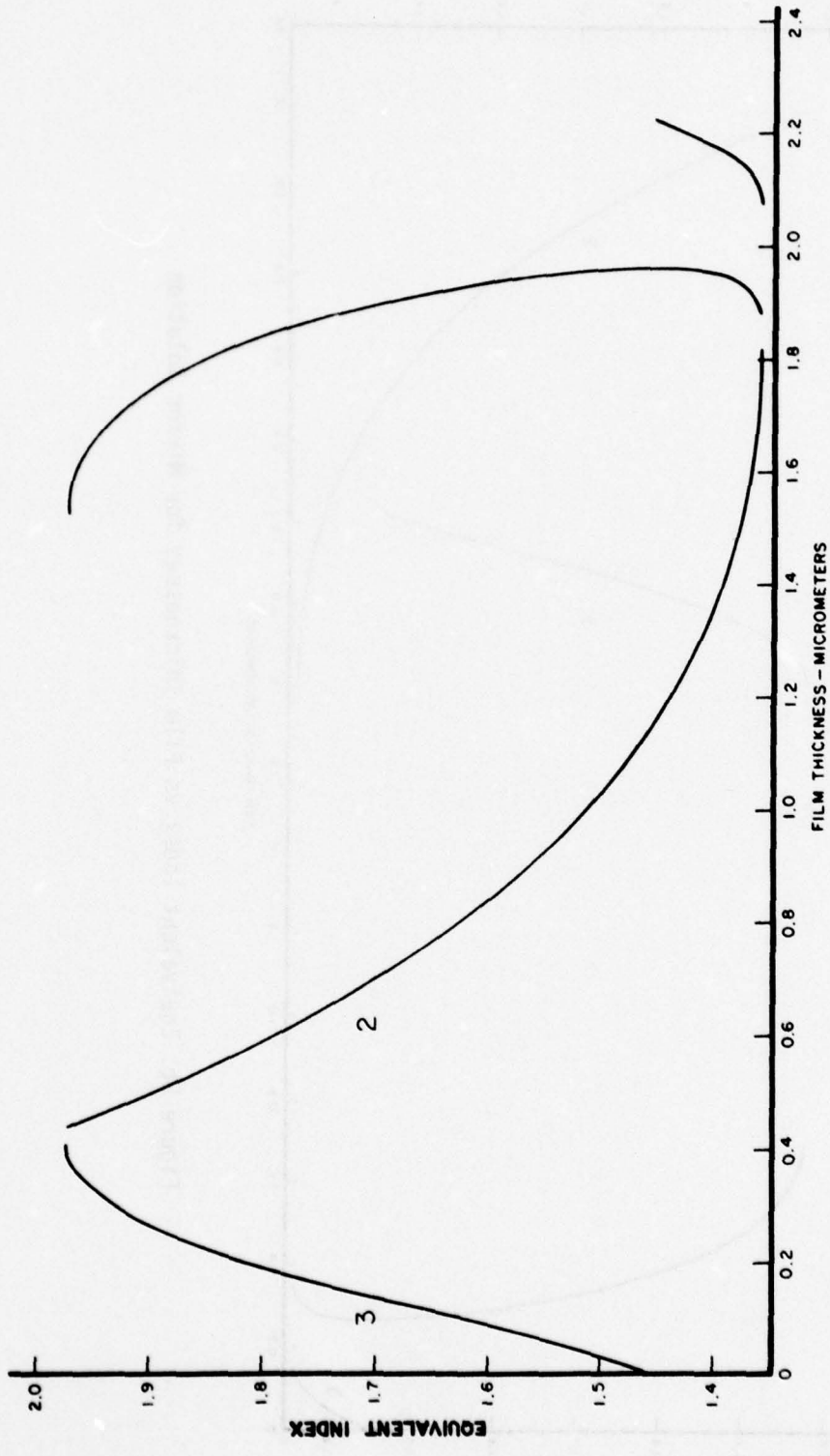


Figure 8a. Equivalent Index vs Film Thicknesses for Thick High Index Solution

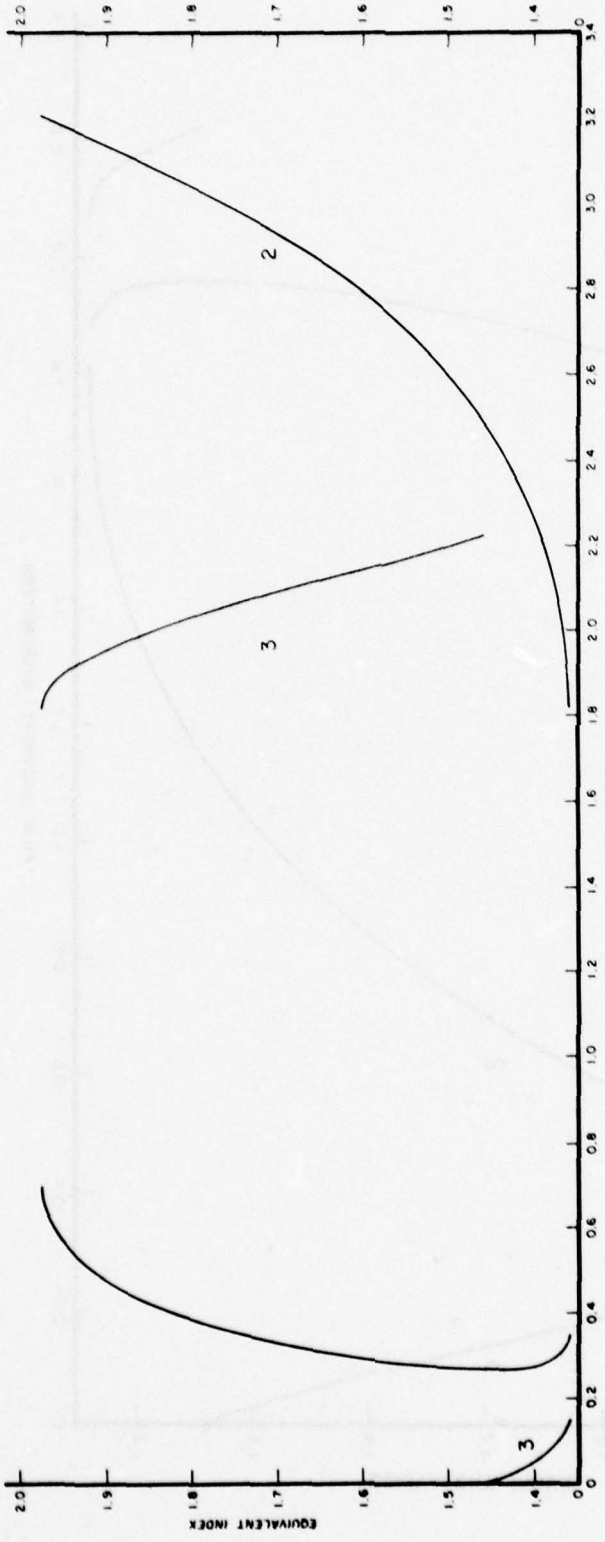
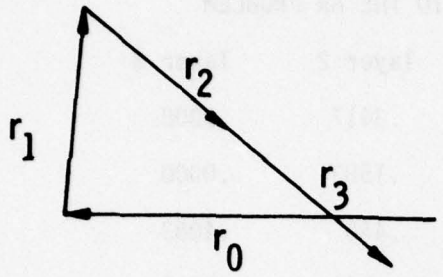
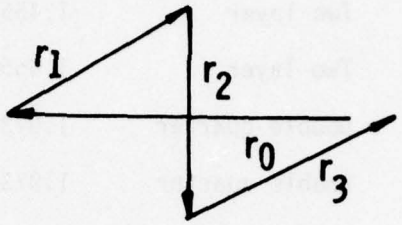


Figure 8b. Equivalent Index vs Film Thicknesses for Mirror Solution



A) Tℓ I / KCl / Tℓ I

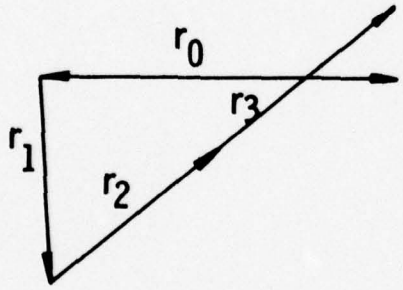
.2479 / .0814 / .1173



B) Tℓ I / KCl / TXℓ I

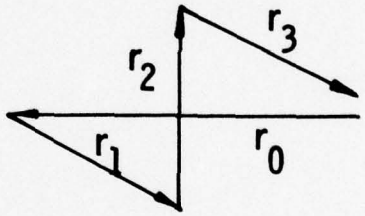
.4125 / .0814 / .0431

N = 1.80



C) Tℓ I / KCl / Tℓ I

.2521 / .4186 / .3827



D) Tℓ I /KCl / Tℓ I

.0875 / .4186 / .4569

Figure 9. Vector Diagrams for Four Solutions for N=1.8: a) $+\theta_2$, $+\sin\mu$, b) $-\theta_2$ $+\sin\mu$, c) $-\theta_2$, $-\sin\mu$, d) $+\theta_2$, $-\sin\mu$. Thicknesses Given in Table.

TABLE 6

SELECTED SPECIAL SOLUTIONS TO THE AR PROBLEM

	N	layer 1	layer 2	layer 3
Two layer	1.455	.0600	.3417	.0000
Two layer	1.455	.440	.1583	.0000
Double quarter	1.973	.1583	.440	.4083
Double quarter	1.973	.3417	.0600	.0917
$+\theta_2$, $+\sin\mu$	1.8	.2479	.0814	.1173
$-\theta_2$, $+\sin\mu$	1.8	.4125	.0814	.0431
$-\theta_2$, $-\sin\mu$	1.8	.2521	.4186	.3827
$+\theta_2$, $-\sin\mu$	1.8	.0875	.4186	.4569

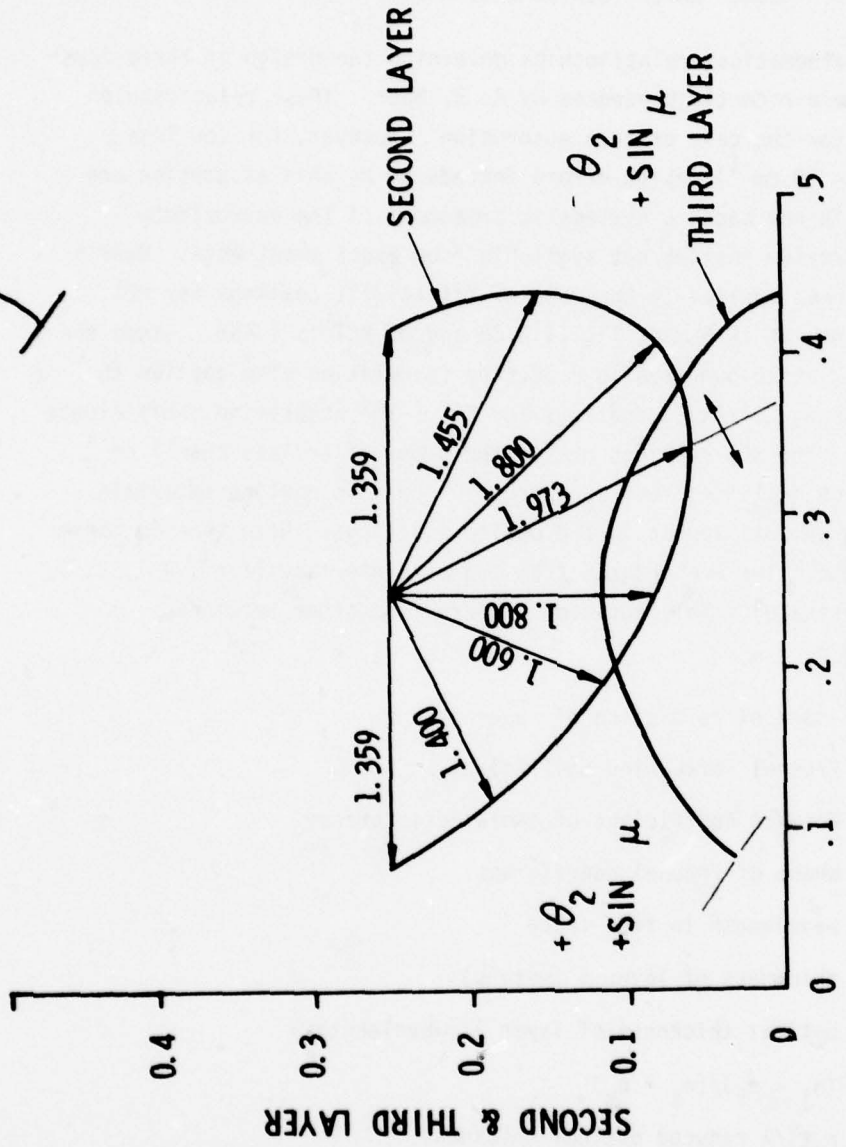


Figure 10. Reduced Optical Thicknesses for Layers 2 and 3 vs. That of Layer 3 in Format of Baer. Radial Lines Indicate Equivalent Index.

SECTION IV

BAER APPROACH TO THREE-LAYER DESIGN FOR MIDDLE LAYER IDENTICAL WITH SUBSTRATE

Simple mathematical relationships governing the design of three-layer AR coatings were recently presented by A. D. Baer. These relationships were derived for the case of zero absorption. However, for low loss materials ($\beta < 10\ cm^{-1}$) design errors introduced by this assumption are negligible. In any case, a systematic treatment of the approximate problem can provide insight not available from exact treatments. Baer's approach has been applied to the case of TlI/KCl/TlI coatings for KCl. The design index at 10.6μm of TlI is 2.38 and of KCl is 1.455. Since the index of As_2S_3 at 10.6μm is also 2.38, the calculation also applies to the case of As_2S_3/KCl/As_2S_3 coatings for KCl. The absorption coefficients of TlI, As_2S_3, and KCl coatings are of the order of or less than 1 cm^{-1} at 10.6μm which qualifies them as extremely low loss coating materials. The following symbols appear in the design equations. Note that in these expressions the films are ordered from the air interface (i.e., A 1, 2, 3, 4 for 4 = substrate). This notation differs from other sections.

$i = -1$

n_j index of refraction of layer j

r Fresnel reflection coefficient

r_{jk} Fresnel coefficient of isolated interface

δ phase of Fresnel coefficient

λ wavelength in free space

t_j = thickness of layer j (meters)

X_j optical thickness of layer j (wavelengths)

r_{jk} $(n_j - n_k)/(n_j + n_k)$

X_j $n_j t_j/\lambda$ reduced optical thickness

N numerator

D denominator

Equations 5-9 for the case of $r_{21} = r_{23} = -r_{34}$ were obtained from Baer. This case applies when the index of layers 1 and 3 are identical and the index of layer 2 is identical to that of the substrate.

$$X_1 = \pm \frac{1}{4\pi} \arccos \frac{r_{21}^2 + r_{10}^2 - |r_b|^2 (1 + r_{21}^2 r_{10}^2)}{2r_{21}r_{10}(|r_b|^2 - 1)} \tag{5}$$

$$X_2 = \frac{1}{4\pi} (\delta_a + \delta_b + 2\pi m) \tag{6}$$

$$m = 0, \pm 1, \pm 2, \ldots$$

$$r_a = \frac{r_{21} + r_{10} \exp(-4\pi X_1 i)}{1 + r_{21}r_{10} \exp(-4\pi X_1 i)} \tag{7}$$

$$r_b = \frac{r_{21} - r_{21} \exp(-4\pi X_3 i)}{1 - r_{21}^2 \exp(-4\pi X_3 i)} \tag{8}$$

Equations 5-11 have been provided to supplement the presentation of Baer.

$$r_b^2 = \frac{2r_{21}^2 - 2r_{21}^2 \cos 4\pi X_3}{1 - 2r_{21}^2 \cos 4\pi X_3 + r_{21}^4} = \frac{N_b^2}{D_b^2} \tag{9}$$

$$r_a^2 = \frac{r_{21}^2 + 2r_{21}r_{10} \cos 4\pi X_1 + r_{10}^2}{1 + 2r_{21}r_{10} \cos 4\pi X_1 + r_{21}^2 r_{10}^2} = \frac{N_a^2}{D_a^2} \tag{10}$$

$$r_k = |r_k| e^{i\delta_k} = |r_k| \cos \delta_k + i|r_k| \sin \delta_k \tag{11}$$

$$\sin \delta_b = \frac{(r_{21} - r_{21}^3) \sin 4\pi X_3}{|r_b| D_b^2} \tag{12}$$

$$\sin \delta_a = \frac{(r_{21}^2 r_{10} - r_{10}) \sin 4\pi X_1}{|r_a| D_a^2} \tag{13}$$

$$\cos \delta_b = \frac{(r_{21} + r_{21}^3)(1 - \cos 4\pi X_3)}{D_b^2 \ |r_b|} \tag{14}$$

$$\cos \delta_a = \frac{r_{21} + r_{21}r_{10}^2 + (r_{21}^2 r_{10} + r_{10}) \cos 4\pi X_1}{D_a^2 \ |r_a|} \tag{15}$$

$$r_a^2 = r_b^2 \tag{16}$$

The required calculations are indicated in the flow chart in Figure 11. The first step is to select an X_3. Only X_3's which are compatible with the appropriate sines and cosines less than or equal to one are permitted. To avoid the requirement of determining the range of X_3 start with an X_3 of 0.25 and decrease by the desired increment to obtain the next X_3. All solutions for X_3 greater than 0.5 can be obtained by subtracting the X_i's for $X_3 \leq .25$ from 0.5. These represent mirror solutions on a circle chart. Since $r_a^2 = r_b^2$ the quantities r_b^2, $|r_b|$, r_a^2, $|r_a|$, and D_b^2 may be obtained from Equation 9. Equation 5 then yields two values for X_1. The quantity D_a^2 from Equation 10 is identical for either value of X_1. The phase angles, δ_a and δ_b, are determined by Equations 12, 13, 14, and 15. Choose δ_a and δ_b to lie between 0° and 360°. The quadrant is determined by Equations 12-15. The angle δ_b is independent of the root of Equation 5. However, δ_a is multivalued with one value associated with each value of X_1. Finally, X_2 is calculated from Equation 6. If X_2 is greater than 0.5 then subtract X_2 from 0.5. The results for X_1, X_2, X_3 for the example under consideration are given in Table 7 and plotted in Figure 12. Designs for any permissible value of X_1 may be accurately determined from Figure 12. Designs for the upper branch of Figure 12 which have very thick layers have not been fabricated. A number of designs for $X_1 \sim 0.3$ have been fabricated since X_2 is very small in that region, an important consideration when the middle layer is a high absorbing material like ThF_4. Designs in the region of $X_3 = 0.09$ -0.15 deserve consideration. As X_3 decreases the bandwidth increases and the total layer thickness of the high index material decreases (very favorable designs for ZnSe which has a residual stress problem).

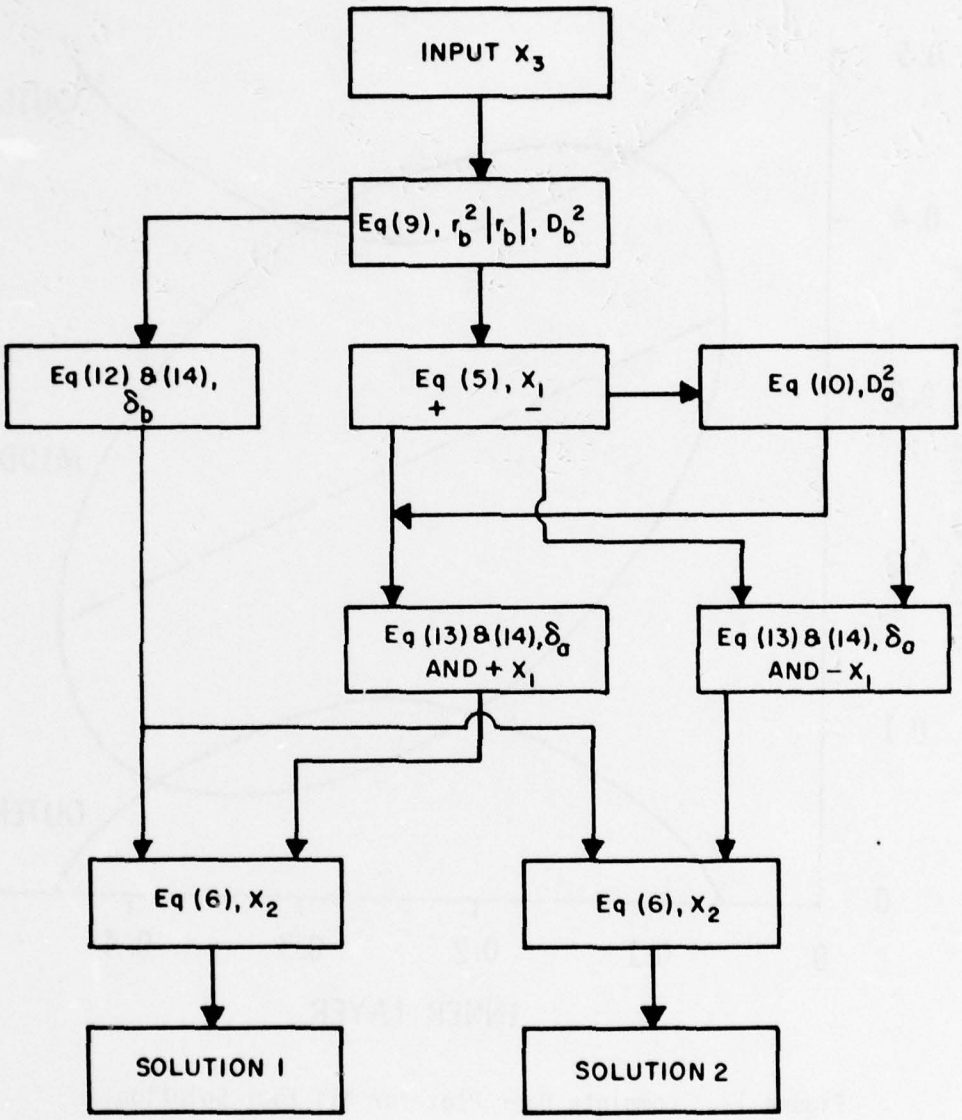


Figure 11. Flow Chart for Baer Calculations.

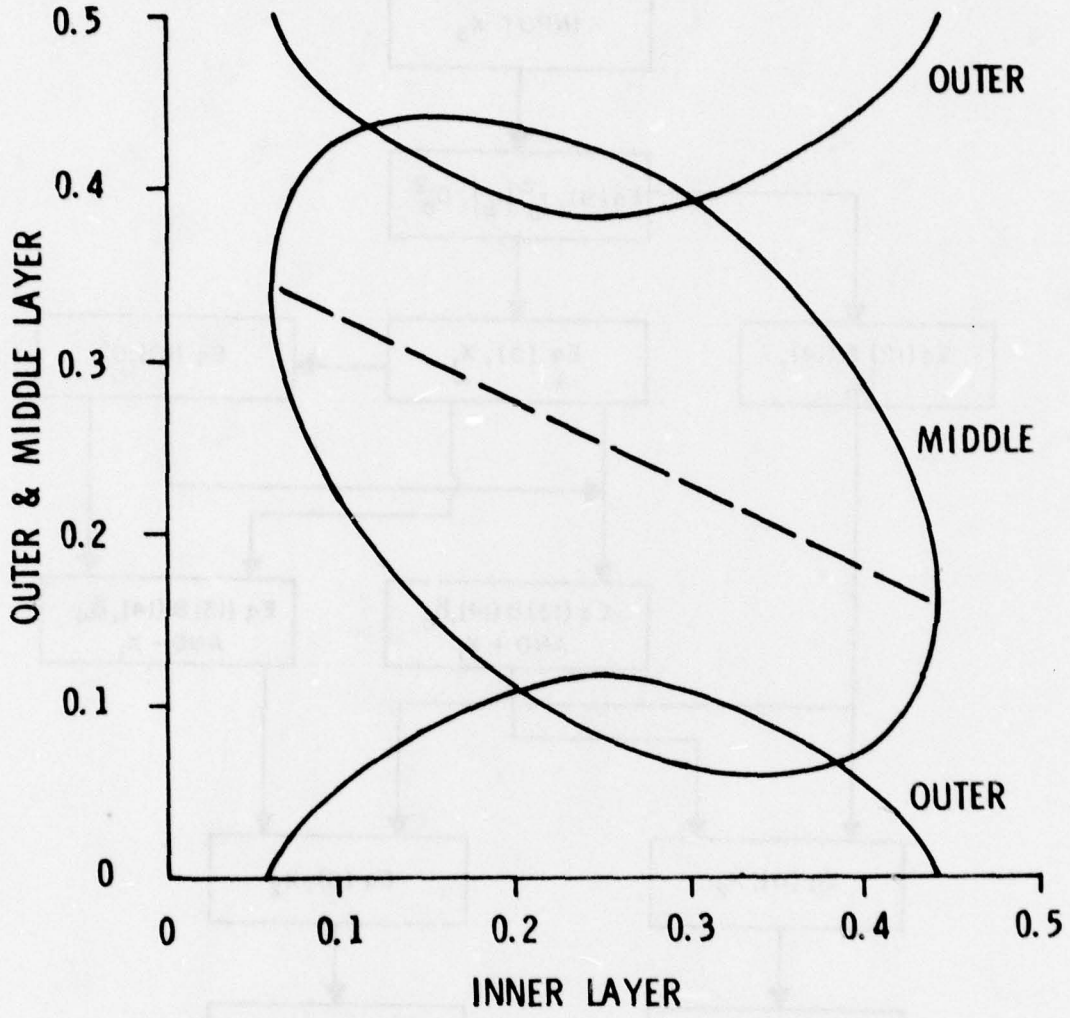


Figure 12. Complete Baer Plot for All Four Solutions.

TABLE 7

REDUCED OPTICAL THICKNESS OBTAINED FROM BAER APPROACH FOR n = 2.38 AND n = 1.455. X EQUALS LAYER 1 ETC.

SOLUTION 1 OR 2	SOLUTION 1		SOLUTION 2	
X_3	X_2	X_1	X_2	X_1
.0590	.3422	.0000	.3422	.5000
.0600	--	--	--	--
.0700	.2778	.0247	.3948	.4753
.0800	.2509	.0361	.4110	.4639
.0900	.2307	.0454	.4207	.4546
.1000	.2138	.0537	.4272	.4463
.1250	.1798	.0719	.4360	.4281
.1500	.1516	.0872	.4397	.4128
.1750	.1285	.0998	.4393	.4002
.2000	.1092	.1093	.4357	.3907
.2250	.0932	.1153	.4279	.3847
.2500	.0805	.1173	.4195	.3827
.2750	.0721	.1153	.4068	.3847
.3000	.0643	.1093	.3908	.3907
.3250	.0608	.0998	.3715	.4002
.3500	.0603	.0872	.3484	.4128
.3750	.0640	.0719	.3202	.4281
.4000	.0728	.0537	.2862	.4463
.4250	.0963	.0307	.2366	.4693
.4410	.1578	0	.1578	.5000

However, since X_1 becomes very thin as X_3 decreases the humidity resistance of the coating may be impaired. TlI/KCl/TlI coatings with a X_3 of 0.16 were found to have a fairly high resistance to damage by high humidity (Reference 5). The trade off of bandwidth and thin high index layers vs. humidity resistance has not been established.

SECTION V

ANHYGROSCOPIC AR COATINGS FOR HALIDES

A proprietary anhygroscopic AR coating for KCl was evaluated with regard to absorption and transmission at 9.27 and 10.6μm. Eight polished polycrystalline Eu++ doped KCl substrates were supplied to the vendor. All eight substrates were coated full aperture on both sides by the vendor.

The substrate properties are described in Table 8. The absorption values were obtained by Honeywell. The strain pattern before and after coating was identical in eight out of eight samples. Under unpolarized light, hints of the substrate strain affected the cosmetics of the coated windows. The coated substrate is water white. It appears that there is no birefringence due to coating strain or orientational preference.

The coatings were designed for 10.6μm. Their transmission as shown in Figure 13a is very broadband. The transmission exceeds 95% for the 7.5 to 12μm region and 90% for the 6.2 to 15μm region. Transmission at 9.28 and 10.6μm is given in Table 9. Figures 13a and b indicate a major change in transmission in sample 1256 after absorption calorimetry. Sample 1260 which was measured nine times in the center has larger bands than 1256 which was measured four times. The calorimeter laser was operated at 20 watts with a beam diameter of 0.4 cm (the standard measurement) which corresponds to ~ 0.2kw/cm. This is the first time at AFML that the absorption of a coated substrate has changed during a calorimeter measurement. Table 10 lists the absorption obtained at the center position for sequential runs on 1260, 1253, and 1256. Note the extremely large absorption which indicates that the reflectivity of the windows is nearly zero. The 9.27μm absorption increases drastically with run number because of the growth of a three peak band. The 10.6μm absorption is relatively constant with a value of 0.7 to 1.1% per surface.

In conclusion, the coating absorption is excessive for high power laser applications. Their performance is modified by 20 watts at 0.2 kw/cm^2. It is possible, because of the lack of band growth at 10.6μm, that the coating would be useful for lasers operating in the 100-watt range or as coatings for halide lenses in IR imaging systems. Since the absorption was excessive for high power laser window applications. environmental tests were not conducted.

TABLE 8

SUBSTRATE PROPERTIES (THICKNESS = 1 cm)

Sample #	Strain Pattern Before Coating	Strain Pattern After Coating	Absorption $10^{-3}cm^{-1}$ (10.6μm)
1253/A-1	Streaks	NC	1.12
1255/A-3	Crosstreaks	NC	.87
1256/A-4	Streaks & Mottled	NC	.91
1259/A-7	Strong Cross-Streaks	NC	.72
1268/A-16	Nonuniformly Mottled	NC	.60
1258/A-6	Nonuniformly Mottled	NC	.88
1260/A-8	Mottled & Boundaries	NC	.67
1262/A-10	Streaks	NC	.71

TABLE 9

WINDOW TRANSMISSION

Sample	Transmission (9.28μm)	Transmission (10.6μm)	Remarks
1253	95.5	98	after calorimetry
1255	95.0	94	before calorimetry
1256	98.8	97.5	before calorimetry
1256	93.0	97.3	after calorimetry
1258	98.0	98.0	before calorimetry
1260	87.0	97.5	after calorimetry
1262	98.0	98.0	before calorimetry
1268	99.0	98.0	before calorimetry

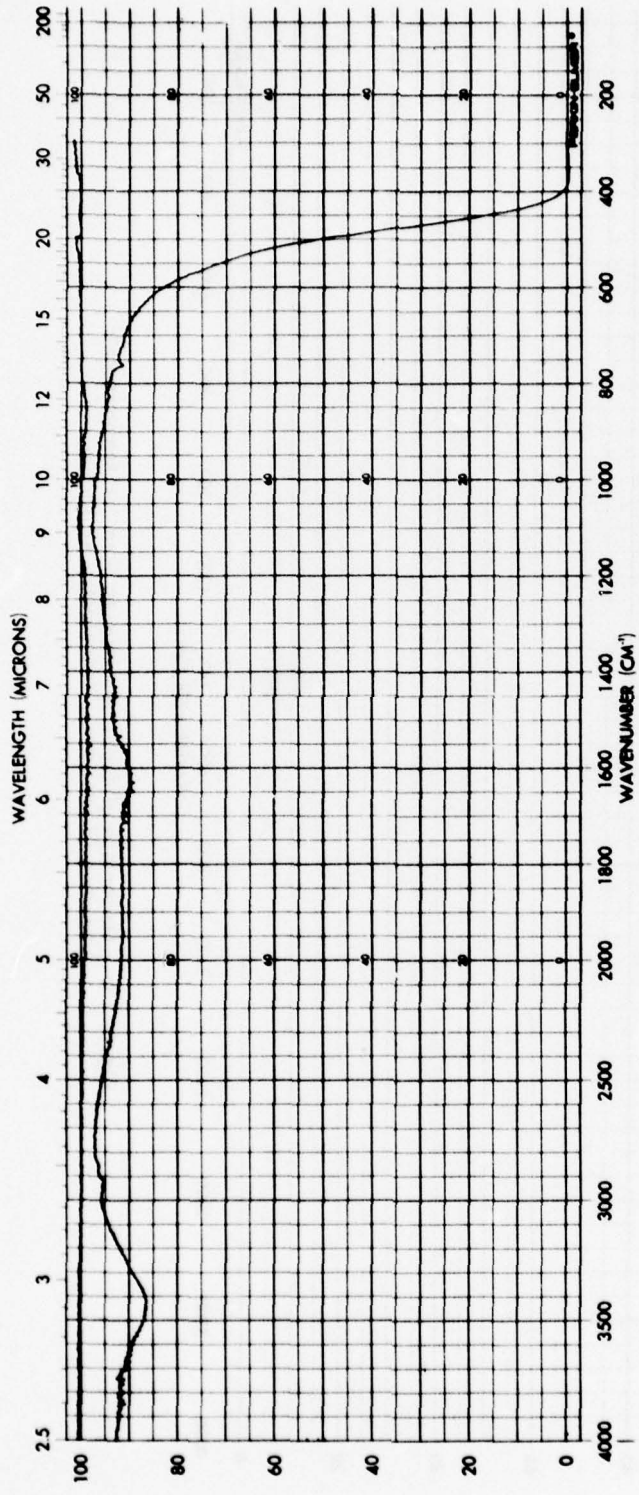


Figure 13a. Comparison of Spectrophotometer Scan for Anhygroscopic Coating (#1256) Before Calorimetry

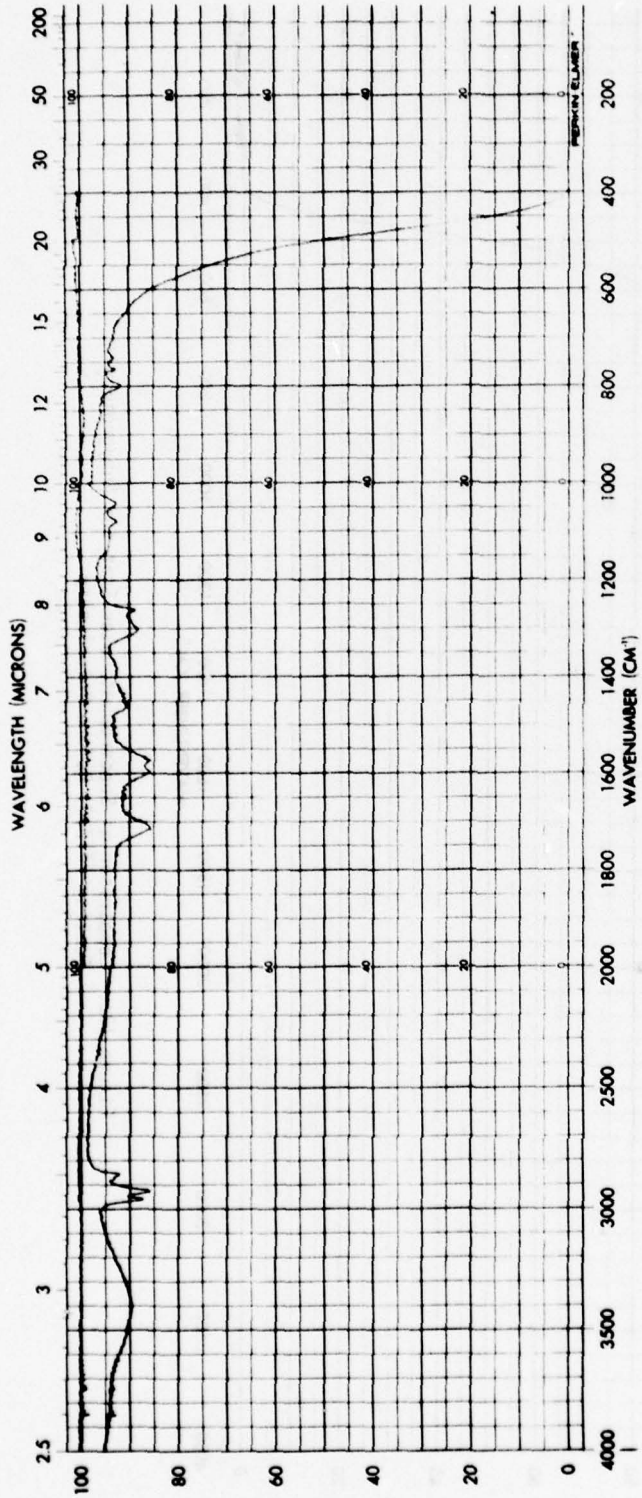


Figure 13b. Comparison of Spectrophotometer Scan for Anhygroscopic Coating (#1256) After Calorimetry at 10.6μm

TABLE 10

COATED WINDOW ABSORPTION

Sample #	Run #	Wavelength (Micrometers)	Total Absorption
1253	1	9.27	2.87%
	2	9.27	4.43%
1260	1	"	2.37%
"	2	"	3.43%
"	3	"	4.95%
"	4	"	6.31%
1260	1	10.6	2.05%
"	2	"	2.28%
"	3	"	2.33%
"	4	"	2.34%
"	5	"	2.32%
1256	1	"	.68%
"	2	"	1.12%
"	3	"	1.3%
"	4	"	1.4%

SECTION VI

EXPERIMENTAL PERFORMANCE OF SOME TlI ANTIREFLECTION COATINGS AT 9.27μm

Seven coating designs were evaluated with regard to absorption, peak transmission, transmission at design wavelength, and damage threshold. The designs are listed in Table 11 and the indices of the coating materials are listed in Table 12. Five samples of Design 1 were supplied by Perkin-Elmer; two of Design 2, four of Design 3, four of Design 6, and two of Design 7 were supplied by OCLI; and five each of Designs 4 and 5 were supplied by Honeywell. Nineteen of the total of 23 samples were of the three-layer type incorporating TlI. The samples are identified in Table 13.

The substrates were polished by the vendors before coating. Since no 9.27μm calorimeters were available, the bulk and the surface absorption of the polished substrates were not measured prior to coating. Honeywell used their standard procedure which produces low absorption surfaces at 10.6μm. OCLI followed a similar procedure. The total absorption for each sample is listed in Table 14. The average absorption in % for Designs 1 through 7 was 0.55, 0.82, 0.54, 0.41, 0.34, 0.70, 4.86, respectively. Designs 4 and 5 can be compared to the state of the art absorption of 0.09% of TlI/KCl/TlI coated KCl at 10.6μm. The excessive absorption at 9.27μm seriously degrades the performance potential of KCl. Focused damage threshold measurements were made on the 9.27μm windows at 10.6μm. The results are shown in Table 15. These thresholds are lower than those previously reported. In prior studies three-layer coatings incorporating TlI had thresholds in excess of 130 kw/cm^2. Transmission vs. wavelength is given in Figures 14a-14f. The bandwidths of Designs 1 and 2 are nearly identical as they should be. Designs 3, 4, and 5 are broader in correspondence with their position on the Baer chart. Some of the initial Honeywell results indicated a reflection per surface of nearly 0.5%. There was speculation that because of scattering and birefringence that zero reflectivity might not be attainable. However, investigation of the present TlI coatings

TABLE 11

THREE-LAYER DESIGNS INVESTIGATED AND THEIR DEPOSITION TEMPERATURE

#	Design	Layer *1	Layer 2	Layer 3	Temperature
1	TlI/ThF_4/TlI	.343 1.327+μ	.056 .368μ	.093 .361μ	100°C
2	TlI/ThF_4/TlI	.349 1.36μ	.057 .38μ	.090 .35μ	100°C
3	TlI/NaF/TlI	.091 .35μ	.157 1.19μ	.065 .25μ	70°C
4	TlI/KCl/TlI	.105 .405μ	.202 1.286μ	.059 .228μ	27°C
5	TlI/KCl/TlI	.219 .844μ	.094 .598μ	.115 .445μ	27°C
6	NaF	.25 1.93μ			175°C
7	CaF_2	.25 1.28μ			100°C

*Reduced Optical Thickness
+Thickness at 9.27μm (2.40 = n of TlI)

TABLE 12

DESIGN INDEX AT 9.27μm

Material	Design	Index
TlI	1	2.40
ThF_4	1	1.40
TlI	2&3	2.40
ThF_4	2	1.40
NaF	3&6	1.20
TlI	4&5	2.40
KCl	4&5	1.455
CaF_2	7	1.30

TABLE 13

SAMPLE IDENTIFICATION

Sample# AFML	VENDOR	Coating Design	Substrate
1748	S/N1	1	Eu-Polytran+
1749	S/N2	1	"
1750	S/N3	1	"
1751	S/N4	1	"
1752	S/N5	1	"
1899	C-1	2	Rb-Polytran+
1900	C-2	2	"
1895	D-1	3	1.75%RbCl*
1896	D-2	3	"
1914	E-1	3	"
1915	E-2	3	"
2295	2-6	4	1.75%RbCl
2296	2-7	4	"
2297	2-8	4	"
2298	2-10	4	"
2299	2-11	4	"
2290	2-1	5	"
2291	2-2	5	"
2292	2-3	5	"
2293	2-4	5	"
2294	2-5	5	"
1911	F-1	6	Rb-Polytran
1912	F-2	6	Rb-Polytran
1918	A-1	6	Rb-Polytran+
1919	A-2	6	"
1907	B-1	7	"
1908	B-2	7	"

TABLE 14

ABSORPTION

Sample#	Coating Design	Substrate Thickness	Total Absorption (%)
1748	1	.805cm	.52
1749	1	.80	.61
1750	1	.805	.51
1751	1	.800	.56
1752	1	.810	.53
1899	2	.625	.85
1900	2	.635	.79
1895	3	.650	.65
1896	3	.610	.41
1914	3	.640	.56
1915	3	.620	.55
2295	5	1.010	.43
2296	5	1.010	.28
2297	5	1.005	.26
2298	5	1.010	.38
2299	5	1.000	.35
2290	4	1.015	.30
2291	4	1.025	.48
2292	4	1.020	.36
2293	4	1.015	.60
2294	4	1.020	.29
1911	6	.625	.73
1912	6	.630	.67
1918	6	.625	.69
1919	6	.635	.72
1907	7	.635	4.46
1908	7	.620	5.26

TABLE 15

FOCUSED DAMAGE THRESHOLDS

Sample#	Design	
1749	1	
1751	1	73kw/cm^2
1895	3	73
1896	3	
1914	3	73
1911	6	73
1912	6	
1918	6	21.6-49
1919	6	

73kw/cm^2 ~ 510 watts

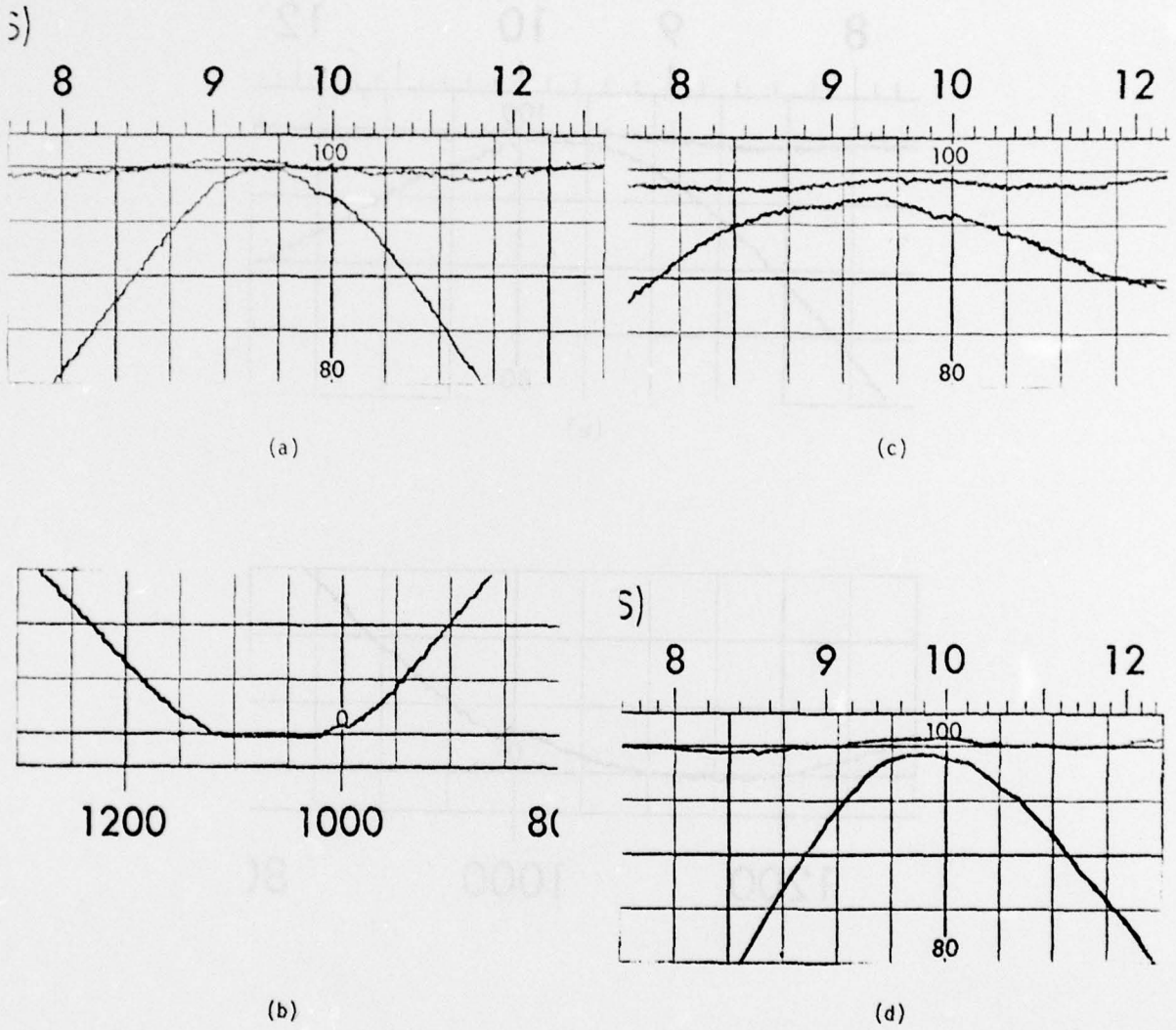
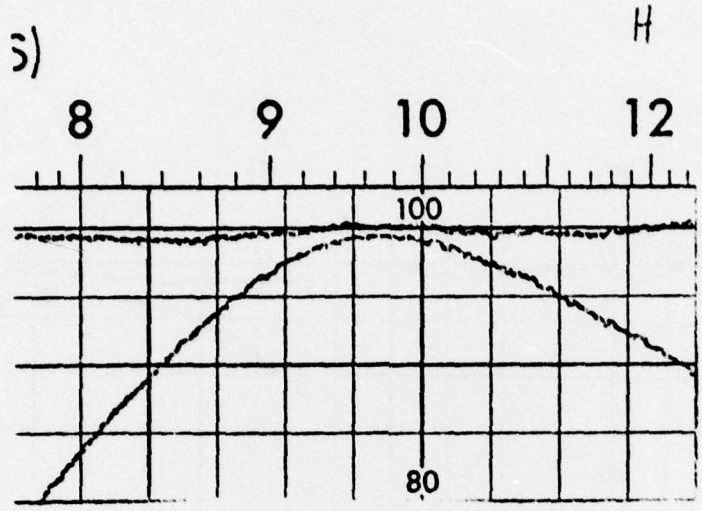
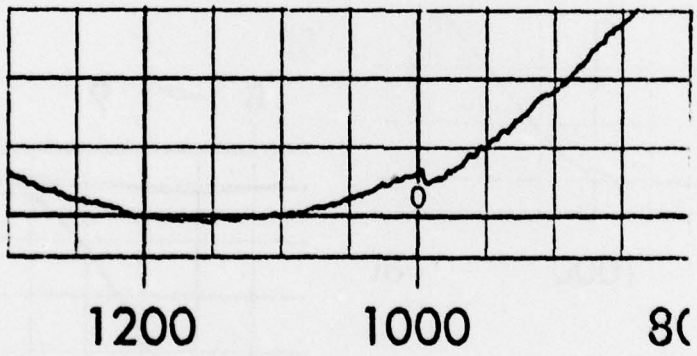


Figure 14. Transmission or Reflection vs Wavelength for Design: a) Design 1 (T) b) Design 2 (R), c) Design 3 (T), d) Design 4 (T), e) Design 5 (T), f) Design 6 (r with KCl in Reference). Vertical Division = 5%; for Transmission Horizontal Axis Is in Micrometers; for Reflection Horizontal Axis Is in Wavenumbers.



(e)



(f)

Figure 14. (Cont'd) Transmission or Reflection vs Wavelength for Design: a) Design 1 (T), b) Design 2 (R), c) Design 3 (T), d) Design 4 (T), e) Design 5 (T), f) Design 6 (R with KCl in Reference). Vertical Division = 5%; for Transmission Horizontal Axis Is in Micrometers; for Reflection Horizontal Axis Is in Wavenumbers.

indicates no inherent material limitation. Although the average reflectance per surface for Designs 4 and 5 was 0.5% at 9.27μm, the minimum reflectances were in the range of 0.03%.

It is interesting to note the Perkin-Elmer used an e-beam source to evaporate TlI and they obtained excellent coatings. It was noted that for a substrate temperature of 140°C the second surface transmission peak would shift, probably due to re-evaporation. A compromise of 100°C was selected since ThF_4 should be deposited on a hot substrate. OCLI investigated a $ZnS/ThF_4/ZnS/ThF_4$ design for KCl and found that crazing of the coating eliminated ZnS as a coating material for KCl. OCLI used 10-minute argon glow discharge and substrate temperatures indicated in Table 11. During an investigation of glow discharge it was found that using N_2 increased absorption (~.6%) and using argon there was no noticeable change. Honeywell does not use glow discharge and their substrate is at room temperature. The question of glow discharge procedure and TlI source cannot be resolved by this study. Perkin-Elmer used a variable wavelength optical thickness monitor operating near one micron and the witness sample approach. Honeywell used a laser monitor operating at 1.15μm and monitored the actual sample. The Perkin-Elmer approach will give a better thickness control in a well calibrated system.

SECTION VII

CONCLUSIONS AND RECOMMENDATIONS

The equivalent film and the Baer approach to antireflection coating design provide a systematic treatment for the approximate problem of zero absorption which can yield valuable insight not available from exact treatments. The equivalent film approach should be extended to consideration of three-layer AR coating designs which do not have zero reflectances. One suggestion might be to begin with the expression for a two-layer reflecting stack. Choose one layer to be identical to either the high or the low index component and synthesize the other layer with an equivalent stack for various reflectance (i.e., .01%, .1%, 1% etc.) At this point in the laser window development program excellent infrared data is available on a number of coating materials. It would be fruitful to use the Baer approach to catalog three-layer coating possibilities for KCl, and CaF_2 in a fashion similar to the Loomis (Reference 23) report on two-layer coatings. The Baer (Reference 22) approach should also be applied to the case of three different coating materials. Wavelength tunable lasers are being incorporated into laser window materials evaluation efforts. Therefore, optical components which have a broadband or multiband response are required. Of particular value would be w-type coatings for 9.27/10.6μm or 2.8/3.8 operation. The equivalent film approach should be used to create a class of such w-coatings consisting of 4, 5 or 6 alternating layers of two different materials following the guidance of Thetford (Reference 24). Some of the Baer designs of three distinct materials can also be broadband and may be identified by Thetford's criteria.

The dramatic increase in absorption in KCl windows at 9.27μm as compared to 10.6μm is evident in the experimental results given in Section VI. Designs 4 and 5 are respectively a factor of 3.8 and 4.6 above the 10.6μm state of the art value of 0.09%. Note that Design 4 with the thicker KCl layer has a substantially higher absorption than Design 5. This result suggests that the design of the TlI/KCl/TlI type with the thinnest KCl layer will have the lowest absorption. It also suggests that KCl films may provide an excellent tool for investigating

the cause of the excessive absorption of KCl at 9.27μm since effect is enhanced in the film ($\beta \approx 20$ cm^{-1}). Absorption of the 10.6μm state of the art coating was obtained at AFML at 9.27μm. The absorption at 9.27μm was up by a factor of 2 for the bare substrates and by a factor of 8 for coated surfaces. Specific results are listed in Table 16. In surveys of materials it has been found that the absorption of ZnS and NaCl at 9.27μm is less than that of 10.6μm indicating more nearly intrinsic behavior. NaCl should therefore be investigated as a replacement film for KCl at 9.27μm. It may be that impurities levels are shifted to a more desirable location in NaCl as compared to KCl.

The bulk absorption of forged KCl is typically 50% higher than the single crystal value at 10.6μm (i.e., $.0004cm^{-1} \rightarrow .0006cm^{-1}$). The bulk absorption of forged KCl at 9.27μm is a factor of 2.5 to 3 times its absorption at 10.6μm. The absorption of mechanically polished KCl can be .001 cm^{-1} or .002 cm^{-1} when the absorption value of the same sample after etching is .0005 cm^{-1}. It is interesting to speculate about the sources of the observed absorptions. W. Harrison has seen an apparent correlation between the sharpness of a 9.9μm (SO_2 = sulfur dioxide) absorption band and the absorption at 9.27μm and 10.6μm. The narrower the band, the lower the absorption at both wavelengths. He has speculated that a highly crystalline impurity site with a well defined resonance is better than an impurity in an amorphous site giving use to a broader band absorption. Such an explanation involving band broadening could account for the enhanced absorption of the mechanically damaged surface in polished KCl and the enhanced absorption of forged KCl through the introduction of broadband impurity absorption at or in the grain boundaries or in the bulk. Another point which should be considered is the behavior of KCl as a center layer in three-layer coatings at 10.6μm. When the center layer thickness in a design is of the order of 0.05 ROT (reduced optical thickness) replacing the highly absorbing ThF_4 center layer by KCl does not reduce the coating absorption. The physical thickness of such a layer is 0.36μ. Possibly interface or surface effects are dominant at such thicknesses again arising from level broadening due to surface states. The interested reader is invited to add additional speculations concerning the source of 9.27μm absorption.

TABLE 16

COMPARISON OF 9.27μm AND 10.6μm ABSORPTION FOR SAMPLES DESCRIBED IN AFML-TR-77-14

Sample #	Substrate Absorption		Per Surface Absorption	
	9.27μ	10.6μ	9.27μ	10.6μ
	(10^{-3} cm^{-1})	(10^{-3} cm^{-1})	%	%
8E2	1.87	1.14	.23	.024
8E3	2.15	.99	.09	.006
8E5	1.94	1.01	.15	.016
8E7	1.75	.97	.11	.02
8F3	1.27	.47	.12	.057
8F5	1.92	.89	.15	.095
8H6	1.35	.60	.10	.012
8H7	2.06	.78	.099	.009

In summary, the coated KCl window absorption at 9.27μm is up by a factor of 3.5 to 4 over the absorption at 10.6μm. A part of the increase can be attributed to the substrate (~ factor of 2). Investigations of the source of the excess absorption in KCl at 9.27μm and in coating materials should be conducted. NaCl has been made in large sizes with a 10.6μm absorption of .0006 cm^{-1}. At 9.27 μm its absorption could be in the range of 1/5 of that value from intrinsic considerations. Therefore, NaCl should be seriously considered as a 9.27μm window material. TlI does not appear to have a 9.27μm absorption problem as indicated by the relative absorptions and relative thicknesses of TlI of Designs 4 and 5. The TlI based AR coating for KCl or NaCl performs well and provides moisture protection. However, an extensive life cycle test/cost program comparing TlI coated halides to coated ZnSe should be conducted. Facilities in high bay areas are now operating with uncoated Brewster halide windows. These windows typically operate for a month with only a bird dirt shield and flow dry nitrogen in Dayton Ohio. Corresponding data for TlI coated KCl in semi-hostile environments is required.

REFERENCES

1. W. B. Harrison, Halide Material Processing for High-Power Infrared Laser Windows, AFML-TR-75-104.

2. W. B. Harrison, Alkali Halide Materials for High-Power Infrared Laser Windows, AFML-TR-76-106.

3. W. B. Harrison, H. Y. B. Mar, W. T. Boord, and J. E. Starling, The Development of Antireflective Thin Films for Polycrystalline Alkali Halide Laser Window Materials, AFML-TR-76-160.

4. J. H. Chaffin, Protective Coatings for Alkali Halide Optical Components, AFCRL-TR-74-0085 (III), 891-898 (1973).

5. W. B. Harrison, H. Y. B. Mar, W. T. Boord, and J. E. Starling, Thallium Iodide Coatings for Potassium Chloride, AFML-TR-77-14.

6. J. A. Detrio, R. D. Petty, M. C. Ohmer, and O. F. Swenson, "AR-Coated KCl Damage at 10.6μm," NBS Special Publication #462, 283-291 (1976).

7. Lem Remho, Private Communication.

8. Richard House, Private Communication.

9. Walt Reichelt, Private Communication.

10. C. J. Duthler, Impurity Absorption in Halide Window Materials, AFML-TR-75-79, 166-171 (1974).

11. L. Skolnik, A. Kahn, R. Brown, H. Lipson, and A. Golubovic, Emittance Studies on Coated Laser Window Materials, AFML-TR-76-83, 805-823 (1975).

12. John R. Kurdock and Edward A. Strouse, Optical Processing of Alkali Halides and Polycrystalline Zinc Selenide for High-Power Laser Applications, AFML-TR-74-166, Part II (1975).

13. M. Braunstein, D. Zuccaro, J. Rudisill, and A. Braunstein, Low Absorption Antireflection Coatings for KCl, AFML-TR-76-83, 135-142 (1975).

14. Gary Blue and Edmund J. Rolinski, "Investigation of Stoichiometry on Optical Properties of Infrared Laser Materials," paper C6 in the Proceedings of the Twenty-Fifth Annual Conference on Mass Spectrometry and Allied Topics, Washington, D. C. 1977.

15. Nils Fernelius, "The Use of Photoacoustic Spectroscopy to Study Laser Window Materials and Thin Film Coatings," Proceedings of 1977 Laser Window Conference, To be Published.

REFERENCES (CONTINUED)

16. J. M. Wimmer, Unpublished Memorandum dated 6 April 1977.

17. R. P. Lowndes and C. H. Perry, "Molecular Structure and Anaharmonicity in Thallium Iodide," J. of Chem Physics, 58, 271-278 (1973).

18. W. Moddeman, Unpublished Memo dated 4 March 1977.

19. Evile Rutner and Paul J. Huffman, "Quantitative Collection of Effluent from a Knudsen Cell for Thin Film Preparation", Technical Memorandum, May 65-5 (1965).

20. Melvin C. Ohmer, Antireflection Coatings/for Calcium Fluoride Laser Windows for 5.3 Microns, AFML-TR-76-103.

21. W. T. Boord, Private Communication.

22. A. D. Baur, "Design of Three-Layer Antireflection Coatings," NBS Special Publication #462, 221-229 (1976).

23. John S. Loomis, Antireflection Coating Designs for 10.6 Micron Window Materials, AFML-TR-72-180 (unlimited distribution), Acc #AD-768 331.

24. A Thetford, "A Method of Designing Three-Layer Antireflection Coatings," Optica Acta, 16, 37-43 (1969).

BIBLIOGRAPHY

THALLIUM-IODIDE REFERENCES

1. Cubicciotti, D., "The Thallium-Iodine Phase Diagram, "J. Less-Common Metals 24, 201-209 (1971).

2. Lowndes, R. P. and Perry, C. H., "Molecular Structure and Anaharmonicity in Thallium Iodide," The Journal of Chemical Physics, 58, 271-278 (1973).

3. Heidrich, K., Staude, W., Treusch, J., and Overhof H., "Optical Properties and Electronic Structure of Simple Cubic and F. c. c. TlI," Solid State Communications, 16, 1043-1045 (1975).

4. Schulz, L. G., "Polymorphism of Cesium and Thallium Halides", Acta Cryst., 4, 487-489 (1951).

5. Berkowitz, J. and Chupka, W. A., "Photoionization of High-Temperature Vapors." I. The Iodides of Sodium, Magnesium, and Thallium," J. of Chem. Phys., 45, 1287-1292 (1966).

6. Sherman, G. H. and Coleman, P. D., "Antireflection Coatings for Silicon in the 2.5-50 μm Region," Applied Optics, 10, 2675-2678 (1971).

7. Moses, A. J., Optical Materials Properties-Handbook of Electronic Materials (Volume I), IFI/Plenum, N. Y., Washington, London (1971).

8. Maier, R. L., et. al., "Infrared Coating Studies, "1st Quarterly Report, Contract DA-44-009-AMC-1707(E), Bausch and Lomb Inc., 16 June 1966-15 September 1966, Access No. 52.

9. Milek, John T., "Data and Literature Survey on Various Properties of Thallium Bromide-Iodide," EPIC Interim Report No. IR-34, Access No. H-600 (1966).

10. Cubicciotti, Daniel, "The Thallium Iodine Phase Diagram," Stanford Research Institute, Contract AT (04-3)-106, Report No. SRIA-106-76, Access No. 64864 mf. (1970).

11. "Toxicity and Pollution Potential of Thallium," V. Zitko 4, Science of Total Environment, 185-192 (1975).

12. O'Connor, J. T. and Sapoznik, A. R., "Biological Cycles for Elements in the Environment and the Neurotoxicity of Metal Alkyls," Proceedings of the Sixteenth Water Quality Conference, 27-33 (1974).

13. Chaffin, J. H., "Protective Coatings for Alkali Halide Optical Components," Third Conference on High-Power Infrared Laser Window Materials, p. 891, AFCRL-TR-74-0085.

BIBLIOGRAPHY (CONTINUED)

14. Chaffin, J. H. and Skogman, R. A., "Thallium Iodide Protective Coatings for Alkali Halide Optical Components," Proceedings of the Fourth Annual Conference on Infrared Laser Window Materials, AFML-TR-75-79, p. 13.

15. Chaffin, J. and Skogman, R., "Thick Coatings of TlI on KCl Substrates for AR Applications," Proceedings of the Fifth Annual Conference on Infrared Laser Window Materials, p. 155, AFML-TR-76-82 (1975).

16. Detrio, J. A., Petty, R. D., Ohmer, M. C., and Swenson, O. F., "AR Coated KCl Damage at 10.6μm," Proceedings of the Eight Boulder Damage Symposium 1976, NBS Special Publication 462, 283-291 (1976).

17. Bernal, E. G., Chaffin, J. H., Koepke, B. G., Maciolek, R. B., and Stokes, R. J., A Study of Polycrystalline Halides for High-Power Laser Applications, Contract DAHC 15-73-C-0464, Honeywell Report HR-76-252-5-26, 1 July 1975 - 31 December 1975.

18. Knox, B. E., and Vedam, K., Coating Science Ellipsometry and Technology, RADC-TR-76-95.

19. Samara, G. A., "Temperature and Pressure Dependence of the Dielectric Constants of the Thallous Halides," Physical Review, 165, 959, (1968).

20. Claudel, J., Hadni, A., and P. Strimer et P. Vergnat, "Spectres D'Absorption et de Reflexion Des Halogenures De Thallium Dans L'Infra-Rouge Lointain A. Basse, Temperature," J. Phys. Chem, Solids, 29, 1539 (1968).

21. Sinton, W. M., and Davis, W. C., "Far Infrared Reflectances of TlCl, TlBr, TlI, Pbs, $PbCl_2$, Zns, CsBr," JOSA 44, 503 (1954).

22. Rodney, W. S., and Malitson, I. H., "Refraction and Dispersion of Thallium Bromide Iodide," Journal of the Opt. Soc. of America, 46, 956 (1956).

23. Chaffin, J. and Skogman, R., Thick Coatings of TlI on KCl Substrates for AR Applications, AFML-TR-76-83, 155-167 (1975).

24. Pearse, R. W. B., Gaydon, A. G., The Identification of Molecular Spectra, 4th Edition, Chapman & Hall, London (1976).

25. Volmer, F., "Uber den Dampfdruck der Halogenide des Thalliums und Bleis," Physikal. Ztschi. 30, 590 (1929).

26. von Wartenberg, H. and Bosse, A., "Der Dampfdruck Einiger Salsye," 28, 384 (1922).

BIBLIOGRAPHY (CONCLUDED)

27. Kelly, K. K., Contributions to the Data On Theoretical Metallurgy Bulletin 383, Part III, The Free Energies of Vaporization and Vapor Pressures of Inorganic Substances, Available NTIS, ACC # Pb189536 (1935).

THICKNESS MONITOR REFERENCES

28. Vermeulen, A. J., "Some Phenomena Connected with the Optical Monitoring of Thin-Film Deposition and Their Application to Optical Coatings," Optica Acta 18, 531-538 (1971).

29. Zabezhinskiy, et al., "Automatic Film Thickness Monitor for Making Multilayer Coatings," 40, 304-307 (1973).

30. Zakharov, Yu. M. and Kuznetsov, A. Ya., "An Equilibrium Point Method for Monitoring Optical Thickness," Optical Technology, 38, 425-427 (1970).

31. Kudryavtseva, A. G., "The Deposition Precision of Two-Layer Antireflection Coatings," 37, 112-113 (1970).

32. Daneu, V., "Optical Thickness, Monitor for Thin Film Deposition," Applied Optics, 14, 962-969 (1975).

33. Pulker, H. K., "Progress in Monitoring Thin Film Thickness with Quartz Crystal Resonators, Thin Solid Films," 32, 27-33 (1976).

COATING REFERENCE

34. Behrndt, Klaus. H., "Film-Thickness and Deposition-Rate Monitoring Devices and Techniques for Producing Film Coatings of Uniform Thickness," Physics of Thin Films, 3, 1-59 (1966).

*U.S.Government Printing Office: 1978 — 757-080/641